JCTC Journal of Chemical Theory and Computation

Article

Cite This: J. Chem. Theory Comput. 2017, 13, 6023−6042

pubs.acs.org/JCTC

Combining Accuracy and Efficiency: An Incremental Focal-Point Method Based on Pair Natural Orbitals

Benjamin Fiedler,[†] Gunnar Schmitz,[‡] Christof Hättig,[¶] and Joachim Friedrich*[,†]

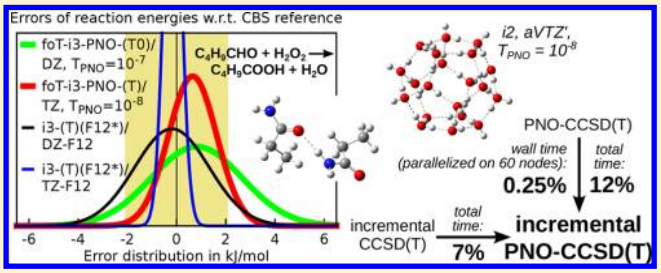
[†]Institut für Chemie, Technische Universität Chemnitz, 09111 Chemnitz, Germany

[‡]Institut for Kemi, Aarhus Universitet, 8000 Aarhus C, Denmark

[¶]Lehrstuhl für Theoretische Chemie, Ruhr-Universität Bochum, 44801 Bochum, Germany

Supporting Information

ABSTRACT: In this work, we present a new pair natural orbitals (PNO)-based incremental scheme to calculate CCSD(T) and CCSD(T0) reaction, interaction, and binding energies. We perform an extensive analysis, which shows small incremental errors similar to previous non-PNO calculations. Furthermore, slight PNO errors are obtained by using $T_{PNO} = T_{TNO}$ with appropriate values of 10^{-7} to 10^{-8} for reactions and 10^{-8} for interaction or binding energies. The combination with the efficient MP2 focal-point approach yields chemical accuracy relative to the complete basis-set (CBS) limit. In this method, small basis sets (cc-pVDZ, def2-TZVP) for the CCSD(T) part are sufficient in case of reactions or interactions, while some larger ones (e.g., (aug)-cc-pVTZ) are necessary for molecular clusters. For these larger basis sets, we show the very high efficiency of our scheme. We obtain not only tremendous decreases of the wall times (i.e., factors $>10^2$) due to the parallelization of the increment calculations as well as of the total times due to the application of PNOs (i.e., compared to the normal incremental scheme) but also smaller total times with respect to the standard PNO method. That way, our new method features a perfect applicability by combining an excellent accuracy with a very high efficiency as well as the accessibility to larger systems due to the separation of the full computation into several small increments.



INTRODUCTION

Since the first ideas by Coester and Kümmel[1,2] as well as its introduction into quantum chemistry by Čížek and Paldus,[3,4] the coupled cluster approach has emerged as one of the most important *ab initio* models for the description of electron correlation. As a wave function-based method, it offers a hierarchical improvability with respect to both the one- and the *N*-electron basis.[5] Especially the coupled cluster method with singles, doubles, and perturbative triples correction (CCSD(T)[6]) has been established as the quantum chemical "gold standard" due to its very high accuracy.[7] However, canonical CCSD(T) features two main disadvantages.

The first one is the slow convergence with respect to the ζ-level of the one-particle basis set.[8] Thus, very large basis sets are required to reach a sufficiently small basis set incompleteness error (BSIE). However, the BSIE can be reduced at rather small computational cost by either CBS extrapolations,[9,10] the application of explicitly correlated methods,[11−14] or the estimation with a lower-level method like MP2.[15−23] The latter approach is simple and very efficient, as the CCSD(T) calculation has to be performed only with a small basis set, but due to an MP2 increment, the results feature the accuracy of the large basis. Recently, this focal-point method has been successfully used in combination with our incremental scheme.[24]

A second disadvantage of canonical CCSD(T) is the unfavorable scaling (O^3V^4) with respect to the number of occupied (O) and virtual (V) orbitals,[6] which limits its application to rather small molecules. Therefore, many approximate methods with a reduced scaling have been developed over the last decades, exploiting the locality of electron correlation.

A first group of these methods is based on the fragmentation of the whole system into smaller units. Here, the total correlation energy is obtained from correlation energy contributions of these units. Examples are the fragment-MO approach of Fedorov, Kitaura, et al.,[25−27] the cluster-in-molecule method (CIM),[28−34] the divide-expand-consolidate (DEC) method,[35−37] natural linear scaling coupled cluster,[38−40] the divide-and-conquer scheme,[41−43] or the EE-MB expansion of Truhlar et al.[44]

Another class of local correlation methods deals with compact representations of the occupied and virtual orbital spaces. Based on the framework of Pulay and Saebø,[45−49] several methods using projected atomic orbitals (PAOs) were implemented by Werner, Schütz et al.,[50−57] by Scuseria and Ayala[58] and by Head-Gordon and co-workers.[59,60] Furthermore, pair natural orbitals (PNOs) have been implemented and

Received: June 22, 2017
Published: October 18, 2017

Downloaded via BOCHUM LIBRARIES on January 16, 2019 at 09:31:38 (UTC).
See https://pubs.acs.org/sharingguidelines for options on how to legitimately share published articles.

© 2017 American Chemical Society

DOI: 10.1021/acs.jctc.7b00654
J. Chem. Theory Comput. 2017, 13, 6023−6042

applied very successfully within the local pair natural orbital (LPNO) and domain-based LPNO (DLPNO) methods of Neese et al.,[61−70] Werner et al.,[71−73] and Hättig, Tew, and co-workers.[74−84]

In our work, we utilize another local correlation method, the incremental scheme, which was originally introduced by Stoll for periodic systems.[85−87] It is based on the generalized Bethe-Goldstone expansion of Nesbet.[88−90] The method was successfully applied to compute energies of periodic systems[91−105] and closed-[106−115] and open-shell[116−119] molecules. Also, molecular properties, like dipole moments,[120] quadrupole moments,[121] and polarizabilities,[122,123] have been calculated.

In this paper, we present a highly efficient and accurate method, which combines our incremental scheme with pair natural orbitals and the focal-point approach. The latter one enables an accuracy close to the CBS limit, while the other two approaches provide a 2-fold reduction of the computational effort. The incremental scheme is known to feature negligible errors with respect to standard CCSD(T), when using a third-order truncation of the incremental series and an MP2-based correction to account for the domain-specific basis set error. The accuracy of the combined method is assessed in this paper, varying different thresholds controlling the accuracy and considering intermolecular interaction and cluster binding energies. Due to the decimated computational effort, we are able to perform CCSD(T) calculations for large molecules. Furthermore, the received method is fully parallelizable in terms of the increment calculations.

THEORY

Incremental Scheme. In the incremental scheme, the total correlation energy is calculated from correlation contributions of fragments (domains) of the complete system.

In a first-order approximation, only the one-site domains are considered. These are disjoint and spatially compact sets of occupied localized molecular orbitals (LMOs), received from a partitioning procedure.[124−126] In that algorithm, occupied Hartree−Fock MOs are Boys-localized,[127] and afterward a graph partitioning as well as a subsequent refinement[128] are performed. The target size of a one-site domain is given by the domain size parameter (dsp), which refers to an approximate number of LMOs in this domain. The number of domains, calculated from dsp, is used in the partitioning to give one-site domains with sizes equal or close to dsp. In previous works, a value of dsp = 4 has been established.[128] Within the domain-specific basis set approach, using the MP2 error correction, this value provides very small local errors, which are not significantly improvable by an increase of dsp. Furthermore, it is small enough to result in a high efficiency.

The correlation contribution of a domain is computed by correlating only the included occupied LMOs. By summing up the one-body increments, that is, the correlation contributions of the one-site domains, a first-order truncation of the incremental series is performed.

For a suitable accuracy of the total correlation energy higher-order increments, that is, nonadditive corrections to the first order, are necessary. Therefore, correlation contributions of N-site domains, which are set unions of N one-site domains, have to be calculated. Within the general expression of an Nth-order increment, which is denoted in eq 1, the subtraction of lower-order increments prevents their multiple counting.[85,124] Here, $\mathcal{P}(\mathbb{X})$ refers to the power set of the orbital set $\mathbb{X}$, which represents a specific N-site domain.

$$\Delta\epsilon_{\mathbb{X}} = \epsilon_{\mathbb{X}} - \sum_{\mathbb{Y}} \Delta\epsilon_{\mathbb{Y}} \quad \{\forall\, \mathbb{Y}\colon \mathbb{Y} \in \mathcal{P}(\mathbb{X}) \wedge |\mathbb{Y}| < |\mathbb{X}|\} \tag{1}$$

In general, these increments decrease with increasing order, which enables the truncation of the incremental series. The total incremental correlation energy of the truncation order O is then obtained by summing up all increments up to this order according to

$$E_{\mathrm{corr}}^{\mathrm{inc}} = \sum_{\mathbb{X}} \Delta\epsilon_{\mathbb{X}} \quad \{\forall\, \mathbb{X}\colon \mathbb{X} \in \mathcal{P}(\mathbb{D}) \wedge |\mathbb{X}| \leq O\} \tag{2}$$

where $\mathcal{P}(\mathbb{D})$ refers to the power set of the set of one-site domains. In most cases, a truncation at third order is sufficient.

The increments also decrease with increasing pairwise distances of the included one-site domains. Therefore, it is reasonable to use an order-dependent truncation distance, $t_{\mathrm{dist}}(i)$, to reduce the number of N-site increments to be calculated. The truncation function in eq 3 with an adjustable parameter f has been utilized successfully in the past,[125,126,129] and a value of f = 30 bohr has been found to allow a truncation without a noticeable loss of accuracy.[128]

$$t_{\mathrm{dist}}(i) = \frac{f}{(i-1)^2} \tag{3}$$

Furthermore, we use the domain-specific basis set approximation[129,130] to reduce the virtual space within the incremental calculations. In this approach, a main region for a specific N-site domain is constructed by the application of a distance parameter t_{main} (see Figure 1). Then all atoms inside the main region are treated in the large target basis set, while a smaller basis (SV) is applied in the environment. Hence, we exploit the fact that virtual orbitals far away from the correlated occupied orbitals are negligible for the description of the correlation effects in the domains.

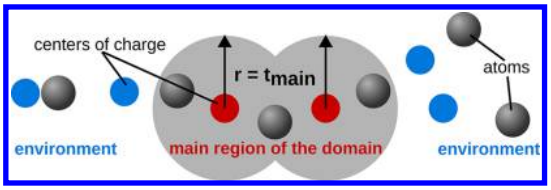


Figure 1. Schematic representation for the construction of the domain-specific basis set. The centers of charge of the considered domain are given in red and their main regions, defined by t_{main}, in light gray. The dark gray atoms in the set union of all main regions are treated with a larger basis set than those in the environment. The centers of charge in the environment are given in blue.

For every domain, SCF orbitals are calculated from a HF calculation with the specific basis set at first. As the initial domain partitioning, which provides all orbitals to be correlated for a specific increment, is done in a small SV basis, the corresponding correlated orbitals in the domain-specific basis set must be identified for every single incremental calculation. Therefore, we map the orbitals in a domain-specific basis to those in the SV basis by a template localization, for which a new implementation has been presented recently.[131]

The introduction of the domain-specific basis set causes an error. It has already been shown that this error can be reduced

DOI: 10.1021/acs.jctc.7b00654
J. Chem. Theory Comput. 2017, 13, 6023−6042

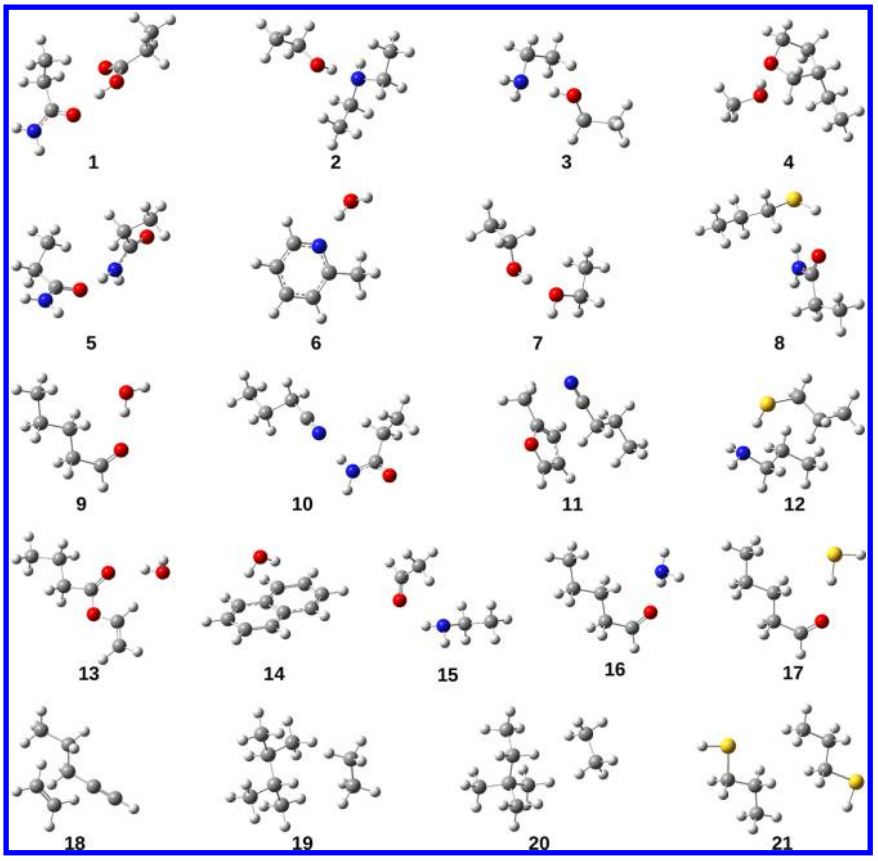


Figure 2. First part of the two-molecule complexes considered in this work. Each consists of two (small- or medium-sized) structures, mainly from the FH test set, and was optimized with BP86-D3/def2-TZVP. The 21 complexes in this figure were used for analyzing the local errors as well as the focal-point approach.

significantly by an MP2-based correction scheme[132,133] according to

$$E_{\mathrm{corr}}^{\mathrm{inc}}(\mathrm{CCSD(T)|MP2}) = E_{\mathrm{corr}}^{\mathrm{inc}}(\mathrm{CCSD(T)}) - [E_{\mathrm{corr}}^{\mathrm{inc}}(\mathrm{MP2}) - E_{\mathrm{corr}}(\mathrm{MP2})] \quad (4)$$

A similar MP2 correction scheme has also been applied by Müller and Usvyat.[120] However, please note that our scheme corrects only for the domain-specific basis set error, that is, it does not correct for a method-specific error due to the incremental expansion itself.[120]

Pair Natural Orbital Approach. The idea of pair natural orbitals (PNOs) was first introduced by Edmiston and Krauss in the 1960s.[134,135] One decade later, Meyer was the first one to implement this concept in context of configuration interaction (CI) and the coupled-electron pair approximation (CEPA).[136−138] Later Ahlrichs, Lishka, Staemmler, and Kutzelnigg picked up this idea in a series of papers,[139−141] but PNOs could not really be established due to the large amount of required PNO integral transformations. However, Neese et al. revisited this approach in 2009 and solved this bottleneck by means of density fitting, which led to a revival of this research field.[61,62]

PNOs enable a tensor factorization of the doubles space. However, beside PNOs the PAO[46,49] and the OSV[142,143] ansatz are other choices for this purpose.

PAOs are generated by orthogonalization of the AOs against the set of (localized) occupied MOs (LMOs). A compressed virtual space for a LMO is often constructed by population analysis in combination with a distance criterion to assign spatially close PAOs to the LMO. For a pair of LMOs *ij*, the PAO sets of *i* and *j* are unified. The error control in this procedure can be unbalanced in some cases, and quite large compressed virtual spaces might be required to ensure sufficiently accurate results. However, the advantage of using PAOs is the requirement of only one integral transformation to the PAO space.

When using PNOs, the virtual space for a given pair *ij* can be further compressed since for each pair of localized occupied orbitals a test wave function is analyzed to construct an optimal specific set of virtuals. Thus, integrals must be transformed for every orbital pair, but compared to PAO-based algorithms, the accuracy and error control is increased.

More recently, the OSVs were introduced by Yang et al.[143] They are somehow a compromise between PAOs and PNOs. The analysis prior to the construction of a specific orbital set is only carried out for each LMO and, according to the PAO case, a pair specific virtual orbital basis is built by unifying the sets for the LMOs.

Most recent local correlation codes feature a strategy of combining these approaches in hybrid schemes, for example, by a prior construction of PAOs or OSVs, so that the subsequent generation of the PNOs is executed in an already truncated doubles space. Such a hybrid OSV−PNO approach is also used in this work. The truncation threshold for the intermediate OSV basis (T_{OSV}) must be adapted to the threshold for the PNOs (T_{PNO}) to preserve their accuracy. In the case of the hybrid approach in this work, a setting of $T_{\mathrm{OSV}} = 0.1T_{\mathrm{PNO}}$ was found to be sufficient to achieve this goal. That way, the threshold T_{PNO} for the truncation of the PNO expansion is in

DOI: 10.1021/acs.jctc.7b00654
J. Chem. Theory Comput. 2017, 13, 6023−6042

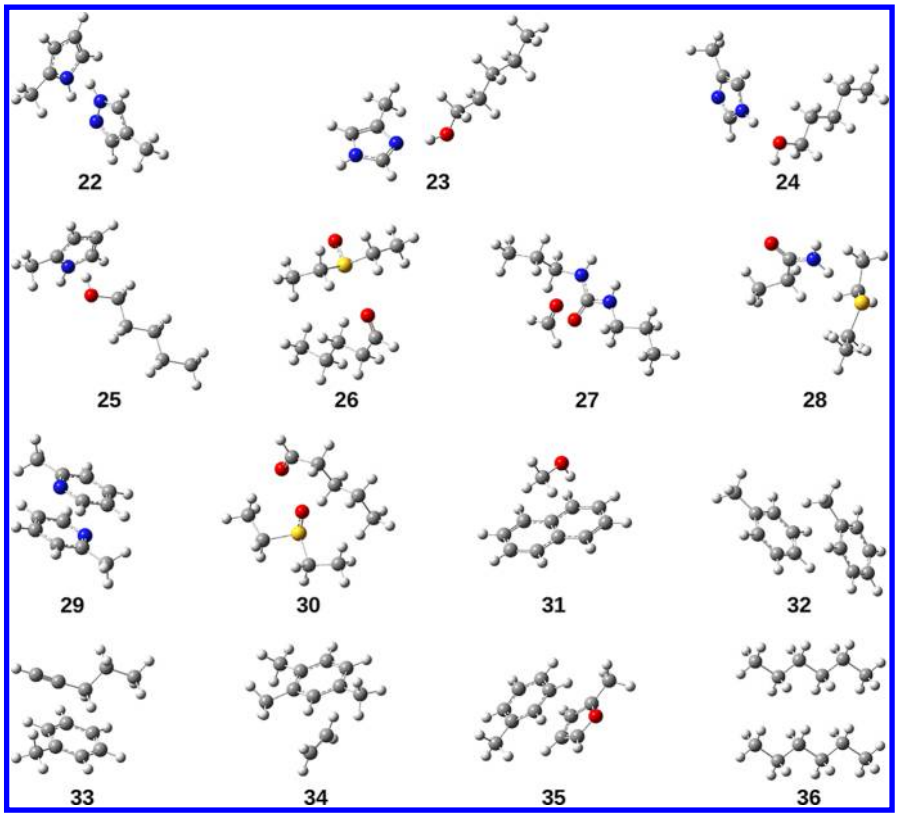


Figure 3. Second part of the two-molecule complexes considered in this work. Each consists of two (small- or medium-sized) structures, mainly from the FH test set, and was optimized with BP86-D3/def2-TZVP. The 15 complexes in this figure were only used for analyzing the local errors but not for the focal-point approach.

principle the only parameter that controls the accuracy of PNO−CCSD and needs to be adjusted. The truncation is based on keeping only those PNOs that feature an occupation number above T_{PNO}. For more information on PNO−CCSD, see ref 62; for details on the construction via the hybrid OSV−PNO approach as well as the corresponding truncation thresholds, see ref 79.

In the spirit of the PNO framework also the triples correction (T) is calculated in a triples specific basis, which was introduced by Riplinger et al. as triple natural orbitals (TNOs).[67] In our current work the construction of this basis is adapted to the hybrid OSV−PNO approach as described in ref 82. Similar to the PNOs, the TNOs are truncated by a threshold T_{TNO}, which controls the accuracy of the triples correction. However, there are two choices for this correction available in the used module: the (T0) approximation, which neglects off-diagonal elements in the occupied−occupied block of the Fock matrix, and the Laplace (T) correction, which accounts for these elements but requires the additional evaluation of integrals at Laplace points for the Laplace quadrature. The number of these points is determined by the Laplace error function, f_{lap}, that is, the number of grid points is increased until $\sqrt{f_{lap}}$ (RMSE of numerical integration) is smaller than a predefined convergence criterion. We refer to the variation of this convergence criterion with *conv X*, where X determines convergence by $\sqrt{f_{lap}} \leq 10^{-X}$. For details on the construction of the TNOs as well as the Laplace triples approach, we recommend again ref 82.

COMPUTATIONAL DETAILS

Test Sets. We tested the performance of our implemented method by means of the FH test set,[128] consisting of 20 small and 81 medium-sized molecules. The incremental scheme was applied only to the latter ones, and the resulting relative energies of 51 corresponding reactions[128] were assessed. These 81 absolute and 51 relative energies have already been considered in previous papers.[131,144]

Furthermore, 36 two-molecule complexes were newly generated from selected molecules of the FH test set (see Figure 2 and 3) to verify also the capability of our method for intermolecular interaction energies. The complexes were optimized on the RI-DFT/BP86-D3/def2-TZVP level of theory as implemented in TURBOMOLE 6.5. Every obtained geometry was characterized as local minimum by means of normal-mode analysis.

The method is also assessed for clusters of small molecules. Therefore, we used a test set of 4 clusters ($(H_2)_{20}$, $(CH_4)_{10}$, $(HF)_{10}$, $(H_2O)_{10}$), which have recently been considered.[24] Furthermore, a $(H_2O)_{20}$ dodecahedron structure from a previous work was also applied.[145]

Statistical and Timing Analyses. For the assessment of the incremental PNO energies, the following reference with a very high accuracy close to the CBS limit[23] has been calculated:

$$E_{ref} = E^{QZ\text{-}F12}_{HF+CABS\text{-}S} + \delta E^{QZ\text{-}F12}_{MP2\text{-}F12} + \delta E^{TZ\text{-}F12}_{CCSD(F12*)} + E^{CBS(23)}_{(T)} \quad (5)$$

with $E_{HF+CABS\text{-}S}$:= Hartree Fock including the CABS-singles contribution, $\delta E_{MP2\text{-}F12}$:= MP2-F12/2B correlation energy, $\delta E_{CCSD(F12*)} = E_{CCSD(F12*)} - E_{MP2\text{-}F12}$, and $\delta E^{CBS(23)}_{(T)} = E^{CBS(23)}_{(T)}$ from eq 6.

DOI: 10.1021/acs.jctc.7b00654
J. Chem. Theory Comput. 2017, 13, 6023−6042

Since the conventional perturbative Triples contribution is usually not sufficient in explicitly correlated coupled cluster calculations,[146,147] the accuracy was improved by a Schwenke type extrapolation[147] according to

$$E_{(T)}^{CBS(23)} = E_{(T)}^{DZ\text{-}F12} + F(E_{(T)}^{TZ\text{-}F12} - E_{(T)}^{DZ\text{-}F12}) \quad (6)$$

with $F = 1.489285$. The upper index denotes the basis set (XZ-F12 := cc-pVXZ-F12). Equation 5 is based on the aim of computing every component with the highest feasible accuracy.

The errors

$$\Delta E_i = E_i(\text{method}) - E_i(\text{ref}) \quad (7)$$

of the absolute and relative energies are given in kJ/mol. Based on these errors, the statistical quantities μ (arithmetic mean error) and σ (standard deviation), as well as MAE (mean absolute error), were computed, and Gaussian error distributions

$$G(x) = \frac{1}{\sigma\sqrt{2\pi}} e^{-1/2((x-\mu)/\sigma)^2} \quad (8)$$

were used for graphical representation.

Besides preserving the accuracy of the parent method, the aim of local correlation methods is a diminution of the computational costs and thus a higher efficiency. Therefore, we also analyzed the timings of our calculation for selected structures, using the total times, t_{total}, according to

$$t_{total} = t_{wall}(\text{server}) + 4 \times \sum_{i=1}^{60} t_{wall}(\text{client } i) \quad (9)$$

for all incremental calculations, which were distributed over 60 client nodes (each with 4 cores) and a server node (using only one core). Each of these nodes is equipped with an Intel Xeon E3-1270 3.4 GHz quad-core CPU and 8 GB RAM. For a better comparability with the incremental timings, we also computed the total times as

$$t_{total} = N_{core} t_{wall} \quad (10)$$

for all nonincremental calculations, which were executed on one node with N_{core} cores (N_{core} = 4 or 12). All calculations with N_{core} = 12 were executed on a node, equipped with two Intel Xeon E5-2620 v3 2.40 GHz hexa-core CPUs and 64 GB RAM. Furthermore, also wall times, t_{wall}, are presented.

Focal-Point Method. In order to reach the complete basis set (CBS) limit of CCSD(T), we use an MP2-based focal-point method[15−23]

$$E(\text{CCSD(T)})_{CBS} = E(\text{CCSD(T)})_{SB} + [E(\text{MP2})_{CBS} - E(\text{MP2})_{SB}] \quad (11)$$

where the large basis set is termed as CBS, as the application of cc-pVTZ-F12 for MP2 results at least in a CBS(45)-extrapolated quality, which is therefore very close to the CBS limit. Furthermore, SB is a small basis. We refer to the method by

$$E(\text{foX-Method}/Y) = E(\text{Method}/Y) + \underbrace{[E(MP2\text{-F12}/\text{XZ-F12}) - E(\text{MP2}/Y)]}_{\Delta E(\text{foX}/Y)} \quad (12)$$

As RI-MP2 is very efficient and features a lower scaling than CCSD(T), this strategy reduces the computational costs significantly. It has been found that a good accuracy can be reached with a triple-ζ basis set as the small one.[148−153] In this work, we test both double- and triple-ζ basis sets within the incremental scheme.

Please note that explicitly correlated coupled cluster methods should be used, if possible, as they improve the wave function ansatz. However, the focal-point ansatz is a computationally less demanding alternative and thus provides access to larger systems.

Incremental and Reference Calculations. All calculations were executed with a development version of the TURBOMOLE program package.[11−13,154−156] We utilized the frozen core approach in all CC and MP2 calculations. Within the incremental scheme, MO coefficients, overlaps, and dipole integrals were received from a modified version of the RICC2 module.[157] Furthermore, we applied the established parameter values dsp = 4, t_{main} = 3 bohr, and f = 30 bohr.[128] We used the SV basis set[158] for the environment of the domains and expanded the incremental series (eq 2) up to the third order. The cc-pVXZ and aug-cc-pVXZ (X = D,T,Q,5)[159−161] basis sets as well as the def2-TZVP[162,163] basis were used as target basis sets.

We utilized a development version of the PNO−CCSD module of Hättig et al. to calculate the increments within our incremental scheme. The Boys localization is used by default. The triples contributions were obtained by both the (T0) approximation and the Laplace ansatz. We varied the parameters T_{PNO}, T_{TNO}, and *conv X*, described in the theoretical section on the Pair Natural Orbital Approach, to adjust them for the use within our incremental method. The OSV truncation threshold, T_{OSV}, within the hybrid approach is set to $0.1T_{PNO}$, by default. The grid points and their weights are determined separately for each increment based on the *conv X* parameter.

The cc-pVXZ-F12 (X = D,T,Q) basis sets of Peterson[164,165] were applied with appropriate CABS[166] to obtain the MP2-based focal-point increments as well as the reference energies. In all explicitly correlated calculations, we used the Slater type correlation factor,[167] represented as linear combination of six Gaussians as implemented in TURBOMOLE,[168] as well as ansatz 2, approximation B,[169] and the fixed amplitude approach.[170] For the correlation factor, we applied the recommended exponents, that is, 0.9 for cc-pVDZ-F12, 1.0 for cc-pVTZ-F12, and 1.1 for cc-pVQZ-F12. The CABS singles correction was added to the Hartree−Fock reference energy.[171,172] Except for the Pair Natural Orbital Approach section, where also uncorrected error contributions are analyzed and separate abbreviations are applied, the notation i3-(PNO)-CCSD(T)/(T0) is used for the third-order (PNO-based) incremental methods with the conventional canonical MP2 correction throughout the complete article.

RESULTS

Parameter Adjustment. In order to optimize our implemented PNO-based method regarding its accuracy and to preserve the very small local errors of the normal incremental scheme, the described parameters, according to the section on the Pair Natural Orbital Approach should be reassessed and, if necessary, readjusted in comparison to the recommendations for the conventional PNO implementation.

Therefore, the dependency on the T_{PNO} parameter was analyzed for the 51 reaction energies of the FH test set at first. T_{TNO} was set to a tight value of 10^{-8} to minimize the truncation

DOI: 10.1021/acs.jctc.7b00654
J. Chem. Theory Comput. 2017, 13, 6023−6042

error for the triples contribution, and the results are presented in terms of mean absolute errors (MAEs) in Figure 4. For comparison, the MAEs of the incremental methods without PNOs are shown as horizontal lines.

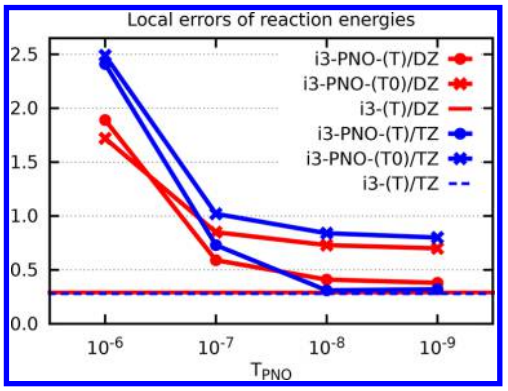


Figure 4. Mean absolute errors of the PNO-based incremental CCSD(T)|MP2 and CCSD(T0)|MP2 reaction energies for the FH test set relative to canonical CCSD(T) with respect to T_{PNO}. Fixed values of $T_{TNO} = 10^{-8}$ and *conv 2* as well as the cc-pVDZ (DZ) or the def2-TZVP (TZ) basis set were used. The MAEs from the normal incremental scheme are shown by horizontal lines.

The convergence with respect to the PNO truncation parameter is well recognizable. Furthermore, the i3-PNO-(T0) curves still provide a deviation from the pure incremental values, even at the convergence limit. This error is due to the (T0) approximation, and the offset appears to be slightly larger than the local errors of the pure incremental scheme, which features MAEs of ≈0.29 kJ/mol for DZ and ≈0.28 kJ/mol for TZ. As the computational cost for the (T0) approximation is clearly lower, it is qualified for a faster alternative with a good accuracy. The Laplace triples correction is clearly more time-consuming but should be the preferred choice due to the higher accuracy. Anyway, for both triples approaches, a value of $T_{PNO} = 10^{-7}$ is sufficient, as the curves are nearly converged, and the MAEs due to the local approximations are about 1 kJ/mol or even slightly lower. With this truncation value, the resulting deviation due to the additional PNO approach is comparable to the pure incremental error. At the convergence limit, which is definitely reached for $T_{PNO} = 10^{-8}$, both (T) curves show a negligible offset from the pure incremental results. This indicates that the PNO error is now small in comparison to the incremental one. Considering the convergence behavior, there are slight differences between both applied basis sets. Compared to cc-pVDZ, the def2-TZVP basis causes a larger deviation from the limit at $T_{PNO} = 10^{-7}$. Thus, if a TZ basis is chosen to obtain a higher accuracy, it may be useful to tighten also the T_{PNO} parameter by one decimal power, that is, to $T_{PNO} = 10^{-8}$. Such a behavior has been explained in ref 74 and was also presented in ref 81. Furthermore, the DZ basis provides a very small offset from the incremental value without PNOs, even at the convergence limit. The reason is the remaining error due to the number of Laplace points, that is, the *conv 2* value. The larger effect of this truncation for cc-pVDZ, in contrast to def2-TZVP (see Figure 6), is presented in the Supporting Information (SI Figure 1).

Please note at this point that the analysis regarding the dependency on T_{PNO} was only performed for the reactions of the FH test set until now, and thus the previous recommendations refer to reaction energies.

In the next step, the accurate calculation of the triples contribution had to be adjusted and therefore the convergence with respect to the truncation value for the TNOs was assessed. The variation of this parameter is presented for the cc-pVDZ basis with $T_{PNO} = 10^{-7}$ and the def2-TZVP basis with $T_{PNO} = 10^{-8}$.

As is evident from Figure 5, the local errors (MAEs) of the reaction energies converge well with T_{TNO}. With the Laplace

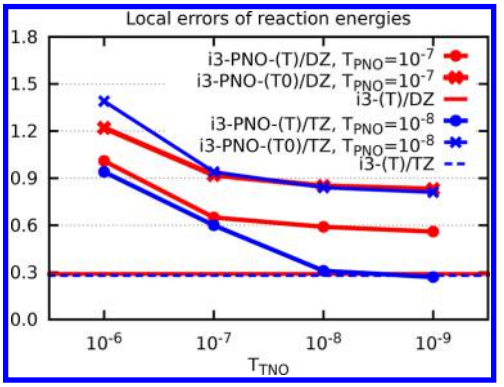


Figure 5. Mean absolute errors of the PNO-based incremental CCSD(T)|MP2 and CCSD(T0)|MP2 reaction energies for the FH test set relative to canonical CCSD(T) with respect to T_{TNO}. The *conv 2* setting as well as the cc-pVDZ (DZ) basis with $T_{PNO} = 10^{-7}$ and the def2-TZVP (TZ) basis with $T_{PNO} = 10^{-8}$ were used. The MAEs from the normal incremental scheme are shown by horizontal lines.

triples, the cc-pVDZ basis and $T_{PNO} = 10^{-7}$ convergence is approximately reached for $T_{TNO} = 10^{-7}$, while $T_{TNO} = 10^{-8}$ is required for def2-TZVP and $T_{PNO} = 10^{-8}$. In case of the DZ basis set, the smaller truncation values explain the difference from the corresponding local error of the incremental scheme without PNOs. For the (T0) approach, $T_{TNO} = 10^{-7}$ is sufficient for both basis sets but there is still an offset from the pure incremental errors due to the approximate triples treatment. However, as a consequence we recommend to set $T_{PNO} = T_{TNO}$ within the PNO-based incremental scheme in any case, similar to the observations of Schmitz and Hättig in context of the standard PNO−CCSD(T) method.[82]

Anyway, accuracy and computational effort of the Laplace triples calculations are also influenced by the number of grid points, which is affected by the convergence criterion (*conv*) of the numerical Laplace transformation. In our incremental scheme, the grid points and the corresponding weights were determined specifically for every increment. For details, see the Pair Natural Orbital Approach section and ref 82. In the previous considerations as well as throughout the complete article, we applied the *conv 2* setting of the Laplace data group within our PNO-based incremental scheme. In order to demonstrate its suitability and to estimate the consequential error, the convergence criterion was also enhanced to *conv 3*. The results for the reaction energies are shown in Figure 6, using the def2-TZVP basis as well as tight parameters ($T_{PNO} = T_{TNO} = 10^{-8}$) to ensure a negligible effect of both truncations.

The graph contains the local error Gaussian distributions, regarding the *conv 1* setting for the Laplace triples (1−2 Laplace points for every increment). In this case, the errors are very large and an increase of the Laplace points is necessary. However, already with the *conv 2* setting (2−3 Laplace points), the triples contribution is significantly improved and chemical accuracy is clearly obtained. Our definition of chemical accuracy

DOI: 10.1021/acs.jctc.7b00654
J. Chem. Theory Comput. 2017, 13, 6023−6042

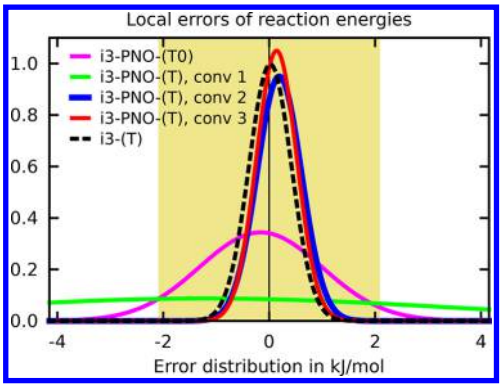


Figure 6. Gaussian error distributions of the PNO-based incremental CCSD(T)|MP2 and CCSD(T0)|MP2 reaction energies for the FH test set relative to canonical CCSD(T). The def2-TZVP basis set and $T_{PNO} = T_{TNO} = 10^{-8}$ were applied. The (T0) approximation and the Laplace approach with different settings of *conv* within the PNO-based scheme as well as the common incremental scheme are compared.

is based on an error interval of 1 kcal/mol width, that is, the interval [−2.1 kJ/mol; +2.1 kJ/mol] (depicted by beige background in Figure 6). To reach this accuracy, the 3σ-interval of a Gaussian distribution, which incorporates about 99.7% of all errors, must be completely inside the 1-kcal/mol-interval. For *conv 2*, a 3σ-interval of [−1.07 kJ/mol; +1.45 kJ/mol] with a width of 2.52 kJ/mol is received, while it is [−1.00 kJ/mol; +1.28 kJ/mol] with a slightly smaller width of 2.28 kJ/mol in case of *conv 3* (mainly 3 Laplace points). With both settings for the Laplace triples, the accuracy of the common incremental scheme is approximately reached, indicating the convergence with respect to the PNO and TNO truncation. Therefore, *conv 2* is in general sufficient due to the obtained high accuracy, which has already been found by Schmitz and Hättig for the conventional PNO−CCSD(T) method with the same setting.[82] Anyway, a slight improvement is still possible, and *conv 3* may be useful in some specific cases (see the section on the Application to Large Systems).

Finally, the recommendations for the assessed parameters in context of our PNO-based incremental scheme correlate well with those for the conventional PNO method, which indicates the suitability of an incremental expansion of PNO energies. However, a more detailed investigation of the local errors is useful and therefore provided in the next section.

Error Analysis. As indicated above, clearer insights into the error contributions due to incremental, PNO, and (T0) approximation are useful to understand the total local errors of the reaction energies. In this context, also the MP2 correction according to eq 4 is considered. From previous works, it is well-known that the incremental CCSD(T) error, which is mainly due to the domain-specific basis set approach, can be appropriately diminished by the MP2 incremental error. For this purpose, that is, to correct only the incremental error, it may be sufficient to use the PNO-MP2 energy as E_{corr}(MP2) contribution in eq 4. We denote this by i3-PNO−CCSD(T)|PNO-MP2 (abbreviated by i3-PNO-(T)|PNO-MP2). Another possibility is the usage of the common correction scheme (as already performed in the Parameter Adjustment section), referred to by i3-PNO−CCSD(T)|MP2 (abbreviated by i3-PNO-(T)|MP2), with canonical MP2 for E_{corr}(MP2). While the first alternative suggests an exclusive correction of the incremental error, the latter one might also correct for the remaining deviation, especially the PNO error. Please note that in this section, i3-PNO-(T) refers to incremental PNO−CCSD(T) energies without any MP2 correction.

However, another error contribution in case of (i3-)PNO−CCSD(T0) is based on the approximate (T0) approach. Therefore, we considered the deviations of (i3-)PNO−CCSD(T0) from the more precise (i3-)PNO−CCSD(T) to estimate the (T0) error. The results for cc-pVDZ and def2-TZVP as well as for truncation thresholds of 10^{-7} and 10^{-8} are denoted in the Supporting Information (SI Table 1) The (T0) errors of the nonincremental methods are nearly independent of the truncation thresholds, basis set size, or incremental treatment. Thus, the (T0) error cannot be influenced noticeably by enhancing thresholds or the basis set and causes a nonvanishing deviation. Therefore, the Laplace triples (T) are again recommended, and further analyses of the PNO and incremental errors are performed for (i3-)PNO−CCSD(T).

The incremental errors in Figure 7 are obtained from the deviations of the incremental PNO or non-PNO reaction

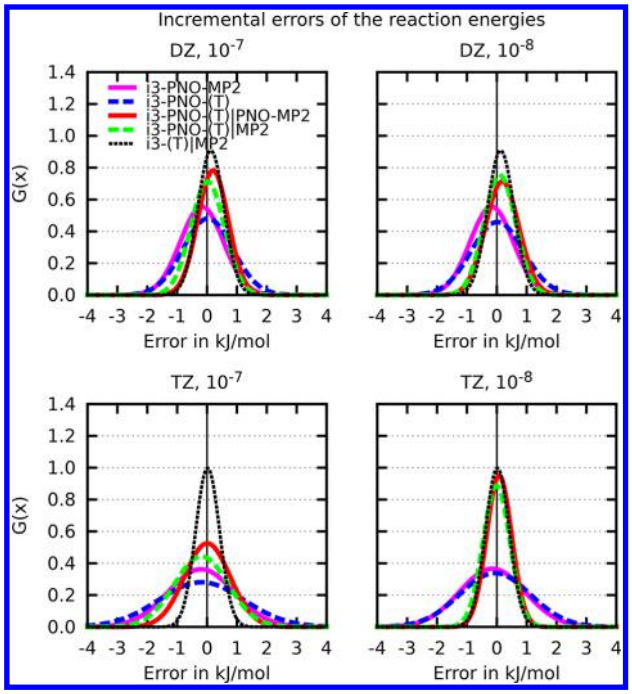


Figure 7. Gaussian error distributions of different incremental approaches with respect to the corresponding nonincremental methods for the reaction energies of the FH test set. The four graphs show the incremental errors for varied basis sets (DZ = cc-pVDZ, TZ = def2-TZVP) and truncation thresholds ($T_{PNO} = T_{TNO} = 10^{-7}$ or 10^{-8}). For the Laplace triples, *conv 2* was used.

energies from their nonincremental counterparts. First, the MP2-corrected incremental errors without PNOs are similar for cc-pVDZ and def2-TZVP basis. Furthermore, the incremental errors of i3-PNO-MP2 and uncorrected i3-PNO−CCSD(T) increase with enlargement of the basis set from DZ to TZ, which is due to the larger differences of main and environmental basis and therefore the increased domain-specific basis set error in the case of def2-TZVP. However, the incremental errors for both methods (PNO−CCSD(T) and PNO-MP2) are very similar. The performance of the MP2 correction is based on this similarity, as the incremental CCSD(T) error is compensated by the corresponding error of PNO-MP2. This can be seen especially for TZ and $T_{PNO} = T_{TNO} = 10^{-8}$, leading to the high accuracy of i3-PNO−CCSD(T)|PNO-MP2. As

DOI: 10.1021/acs.jctc.7b00654
J. Chem. Theory Comput. 2017, 13, 6023−6042

previously discussed, the PNO-MP2 energy is suitable to correct for the domain-specific basis set error of i3-PNO−CCSD(T) and the correction with canonical MP2 leads to similar or even worse incremental errors. However, the correction with MP2 instead of PNO-MP2 may improve the total accuracy due to a reduction of the PNO error. Finally, considering the truncation thresholds, the incremental error does not significantly change from 10^{-7} to 10^{-8} for the cc-pVDZ basis, while it is clearly decreased for def2-TZVP. Thus, also with regard to the incremental error, the truncation with $T_{PNO} = T_{TNO} = 10^{-7}$ is sufficient for DZ, and again 10^{-8} is recommended for TZ.

Next, the deviations of the PNO-based (incremental and nonincremental) reaction energies from the corresponding results without PNOs are considered in Figure 8. For all

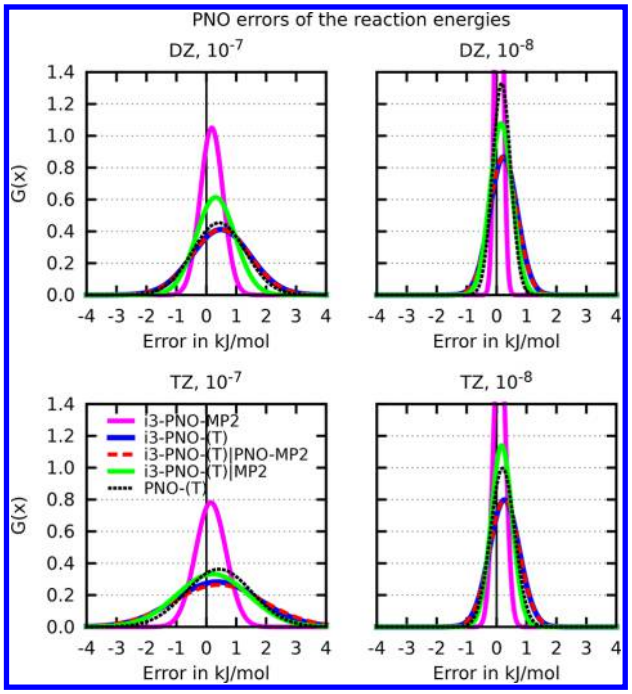


Figure 8. Gaussian error distributions of different PNO-based approaches with respect to the corresponding methods without PNOs for the reaction energies of the FH test set. The four graphs show the PNO errors for varied basis sets (DZ = cc-pVDZ, TZ = def2-TZVP) and truncation thresholds ($T_{PNO} = T_{TNO} = 10^{-7}$ or 10^{-8}). For the Laplace triples, *conv 2* was used.

approaches, these PNO errors decrease with the tightening of the truncation thresholds from 10^{-7} to 10^{-8}. Furthermore, they are slightly larger for i3-PNO−CCSD(T) compared to the nonincremental PNO−CCSD(T). The application of the PNO-MP2 correction scheme does not improve the accuracy of i3-PNO−CCSD(T), which is consistent with the previous discussion on the exclusive correction for the incremental error. In contrast, the common MP2 correction provides a higher accuracy than the uncorrected i3-PNO−CCSD(T), that is, a slight reduction of the PNO error within CCSD(T) by the corresponding error of MP2 occurs. However, this enhancement is less extensive than the decrease of the incremental errors by the MP2 correction. The reason is the larger difference between the PNO errors of the incremental MP2 and CCSD(T) methods, that is, a minor similarity in comparison to the incremental errors in Figure 7. The PNO errors of i3-MP2 are clearly lower than those of i3-CCSD(T).

Basically, the PNO and incremental errors feature comparable dimensions (see Figure 7), but there are some differences, depending on the truncation thresholds and the basis set. For $T_{PNO} = T_{TNO} = 10^{-7}$, the PNO errors are somewhat larger than the incremental ones. For cc-pVDZ and 10^{-8}, the PNO error is now smaller than the incremental error, while def2-TZVP with the same truncation features nearly equal contributions.

Although the incremental and PNO errors have only been considered for the Laplace ansatz, the total local errors of the PNO-based incremental reaction energies with (T0) triples are additionally presented in the Supporting Information (SI Figure 2). They provide wider distributions, and the tightening of the truncation thresholds from 10^{-7} to 10^{-8} leads to smaller decreases of the local errors, compared to the Laplace ansatz. That way, chemical accuracy cannot be reached by the (T0)-based methods. In case of the Laplace triples, the better performance of the MP2 correction in comparison to the PNO-MP2 scheme due to the additional partial compensation of the PNO error is recognizable. For the PNO/TNO truncation with 10^{-7}, the accuracies of i3-PNO−CCSD(T)|MP2 and PNO−CCSD(T) are very similar for both basis sets, as the incremental error contribution is relatively small and the PNO error is determining the total local error. In case of the cc-pVDZ basis set, the tightening to $T_{PNO} = T_{TNO} = 10^{-8}$ clearly decreases the PNO error, that is, the local error of PNO−CCSD(T). However, the accuracy of the i3-PNO−CCSD(T)|MP2 method is less improved, since the incremental error remaining after MP2 correction is now slightly determining. Therefore, again truncation thresholds of 10^{-7} are sufficient for the smaller DZ basis. In contrast, the tighter truncation is useful for def2-TZVP. With this approach, the PNO error, the incremental error, and the local error of the resulting i3-PNO−CCSD(T)|MP2 method are very similar and clearly provide chemical accuracy (Figure 9).

Interaction Energies. In order to show the wide applicability of the PNO-based incremental scheme, intermolecular interactions were also treated with this method. The local errors of interaction energies were analyzed by means of 36 complexes (see Figures 2 and 3).

Again, the convergence of the local errors with respect to the truncation parameter for the PNOs was examined for the cc-pVDZ and the def2-TZVP basis by means of the MAE. Figure 10 shows that the convergence behavior for both basis sets is quite similar to a slightly stronger decrease for def2-TZVP. In comparison to the reaction energies (FH test set, see Figure 4), the convergence of the local error with respect to T_{PNO} is slower for the interaction energies. Therefore, the truncation thresholds should be chosen somewhat tighter for intermolecular interactions to preserve a very high accuracy, and we recommend to use at least $T_{PNO} = 10^{-8}$ (and thus also $T_{TNO} = 10^{-8}$) in any case, even for the smaller DZ basis. Within a recent study on the accuracy of (explicitly correlated) conventional PNO, Schmitz and Hättig obtained similar results regarding the truncation adjustment for weak intermolecular interactions.[84]

Next, Table 1 shows the statistical quantities of the local errors for the incremental and nonincremental PNO interaction energies, using the recommended value of 10^{-8} for both truncation parameters. In general, the errors are similar with no clear order for cc-pVDZ and def2-TZVP and slightly smaller errors for the Laplace triples (compared to the (T0) approximation). Furthermore, they provide nearly chemical

DOI: 10.1021/acs.jctc.7b00654
J. Chem. Theory Comput. 2017, 13, 6023−6042

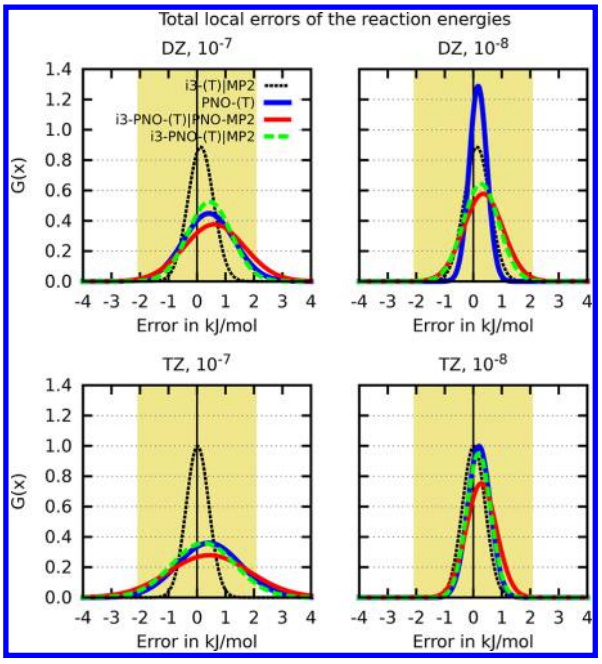


Figure 9. Gaussian error distributions of different CCSD(T) approaches (common incremental, conventional PNO, PNO-based incremental) with respect to the canonical CCSD(T) for the reaction energies of the FH test set. The four graphs show the total local errors for varied basis sets (DZ = cc-pVDZ, TZ = def2-TZVP) and truncation thresholds ($T_{PNO} = T_{TNO} = 10^{-7}$ or 10^{-8}). For the Laplace triples, *conv 2* was used.

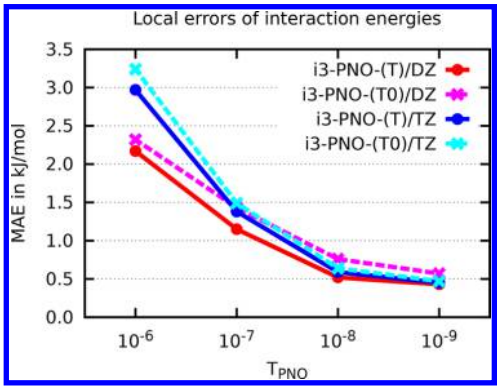


Figure 10. Mean absolute errors of incremental PNO−CCSD(T) and PNO−CCSD(T0) interaction energies for the complexes in Figures 2 and 3 relative to canonical CCSD(T). Fixed values of $T_{TNO} = 10^{-8}$ and *conv 2*, as well as the cc-pVDZ (DZ) or the def2-TZVP (TZ) basis set, were used.

Table 1. Statistical Quantities (in kJ/mol) Regarding the Local Errors of Incremental and Conventional PNO-Based Interactions Energies for the Test Set of Complexes[a]

	μ		σ		MAE	
	i3-PNO	PNO	i3-PNO	PNO	i3-PNO	PNO
DZ,(T)	+0.39	+0.34	0.71	0.37	0.52	0.40
DZ,(T0)	+0.75	+0.74	1.00	0.33	0.76	0.74
TZ,(T)	+0.51	+0.60	0.62	0.29	0.59	0.60
TZ,(T0)	+0.61	+0.90	0.70	0.41	0.64	0.90

[a]See Figures 2 and 3. Fixed values of $T_{PNO} = T_{TNO} = 10^{-8}$ and Laplace triples (T) with *conv 2* or (T0) triples as well as the cc-pVDZ (DZ) or the def2-TZVP (TZ) basis set were used.

accuracy. The incremental methods feature clearly larger standard deviations than the corresponding nonincremental PNO ones but provide comparable mean deviations and MAEs. Therefore, the incremental expansion causes a larger variance but no significant additional errors (see also Figure 11). Both the incremental and the nonincremental distributions feature a positive offset, indicating that the extent of the interaction energies is underestimated on average.

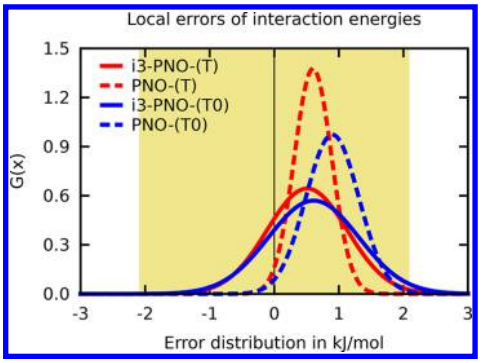


Figure 11. Gaussian error distributions of the conventional and incremental PNO−CCSD(T) and PNO−CCSD(T0) interaction energies for the test set of complexes relative to canonical CCSD(T). Fixed values of $T_{PNO} = T_{TNO} = 10^{-8}$ and *conv 2* as well as the def2-TZVP basis set were used.

Focal-Point Approach. At this point, we have analyzed and adjusted our PNO-based incremental scheme in a way that we can calculate relative energies with very small local errors. However, to reach a high overall accuracy, we have to get closer to the CBS limit. An efficient way is the focal-point approach according to eq 12, which we utilized for both reaction (Figures 12 and 13) and interaction energies (Figure 14). The

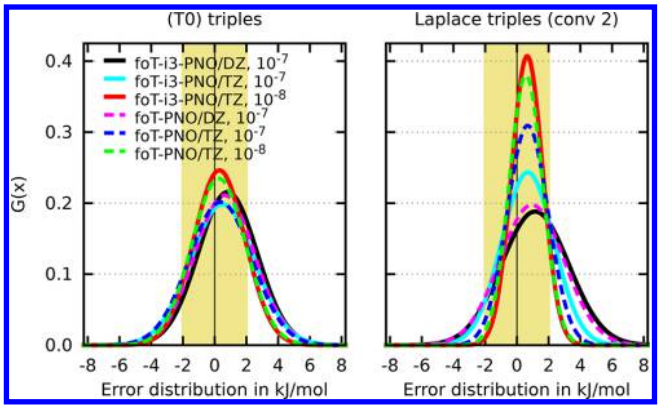


Figure 12. Gaussian error distributions of focal-point incremental and nonincremental PNO−CCSD(T0) (left) and PNO−CCSD(T) (right) reaction energies for the FH test set relative to eq 5. Different basis sets (DZ = cc-pVDZ, TZ = def2-TZVP) and truncation values (10^{-7}, 10^{-8}) as well as *conv 2* were used.

performance of this approach is based on correcting the CCSD(T) results in a small basis with an MP2 increment that reduces the basis set error (see Figure 14).

Figure 12 shows the error distributions of the PNO-based incremental CCSD(T) and CCSD(T0) methods. For the (T0) approaches (left), the different settings provide nearly the same accuracy, that is, the less-demanding cc-pVDZ calculation with $T_{PNO} = T_{TNO} = 10^{-7}$ is sufficient when using this cheaper

DOI: 10.1021/acs.jctc.7b00654
J. Chem. Theory Comput. 2017, 13, 6023−6042

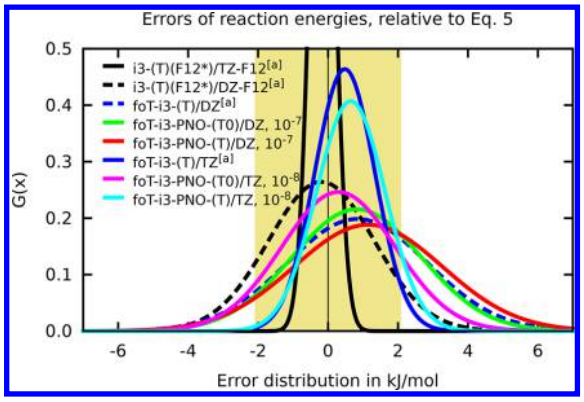


Figure 13. Gaussian error distributions of focal-point incremental PNO−CCSD(T) and PNO−CCSD(T0) reaction energies for the FH test set relative to eq 5. Different basis sets (DZ = cc-pVDZ, TZ = def2-TZVP) and truncation values (10^{-7}, 10^{-8}), as well as *conv 2* were used. [a]Comparison to conventional focal-point and explicitly correlated incremental methods from refs 128 and 131.

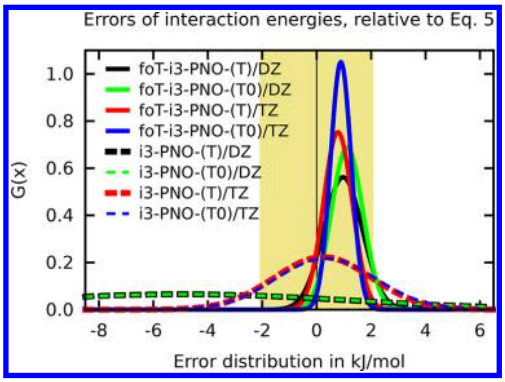


Figure 14. Gaussian error distributions of focal-point and nonfocal incremental PNO−CCSD(T) and PNO−CCSD(T0) interaction energies for the complexes in Figure 2 relative to eq 5. Different basis sets (DZ = cc-pVDZ, TZ = def2-TZVP) as well as $T_{PNO} = T_{TNO} = 10^{-8}$ and *conv 2* were used.

approximation. It is even slightly more accurate than the foT-i3-PNO−CCSD(T)|MP2 approach with the same setting, applying the Laplace triples. Furthermore, the deviations of incremental and standard PNO method are negligible.

The error of foT-i3-PNO−CCSD(T)|MP2, that is, with Laplace triples and the *conv 2* setting (right), is improved by def2-TZVP instead of cc-pVDZ as small basis set as well as by the further tightening of the truncation parameters from 10^{-7} to 10^{-8}. That way, foT-i3-PNO−CCSD(T)|MP2 based on the def2-TZVP basis and with $T_{PNO} = T_{TNO} = 10^{-8}$ features an error distribution close to chemical accuracy. In order to examine the influence of the incremental expansion, the graph shows also the conventional PNO methods in combination with the focal-point treatment. While the deviation from the corresponding incremental curve is negligible for cc-pVDZ/10^{-7} and def2-TZVP/10^{-8}, it is recognizable for def2-TZVP/10^{-7} but also clearly smaller than the effect of tightening the truncation threshold. Thus, the minimal additional incremental error is again demonstrated.

Next, Figure 13 gives a comparison of our PNO-based incremental focal-point approach with standard incremental methods, assessed in a previous work.[131] When using the def2-TZVP basis with truncation values of 10^{-8} or the cc-pVDZ basis with 10^{-7}, our scheme with Laplace triples provides nearly the same distribution as the corresponding conventional incremental method, that is, without PNOs. With (T0) triples even a slightly higher accuracy is reached in case of the cc-pVDZ basis. While the focal-point approach for def2-TZVP causes a broader error distribution, when using 10^{-7} as truncation parameter, the tightening to 10^{-8} nearly leads to chemical accuracy. The foT-i3-PNO−CCSD(T)|MP2/def2-TZVP method ($T_{PNO} = T_{TNO} = 10^{-8}$) features an accuracy between those of incremental (non-PNO) explicitly correlated calculations with a cc-pVDZ-F12 and a cc-pVTZ-F12 basis. But one has to keep in mind, that the computational effort of the PNO-based incremental def2-TZVP calculation is lower than that for an incremental explicitly correlated calculation in the DZ-F12 basis, already for medium-sized systems. Thus, it is also significantly faster than an incremental calculation in the TZ-F12 basis.

The focal-point approach was also assessed for a subset of 21 interaction energies (Figure 2), and the results for the tight setting of $T_{PNO} = T_{TNO} = 10^{-8}$ are presented in Figure 14. First, the increased total accuracy due to the focal-point approach is demonstrated for both basis sets. While the broad nonfocal distributions represent the rather large basis set incompleteness errors, their estimation at the MP2 level leads nearly to chemical accuracy of the interaction energies. However, all focal-point methods feature a positive offset, that is, the (negative) intermolecular interactions tend to be underestimated. In comparison to the Laplace triples, the (T0) approximation provides a similar accuracy, that is, even a slightly tighter distribution but a somewhat larger offset. The same behavior is recognizable for the cc-pVDZ basis but with little worse distributions. However, the focal-point approach in combination with our PNO-based incremental scheme could also be established as a very accurate method to calculate intermolecular interaction energies. If, for example, the def2-TZVP is used as small basis set together with $T_{PNO} = T_{TNO} = 10^{-8}$ and *conv 2*, we obtain $\mu = 0.78$ kJ/mol and $\sigma = 0.53$ kJ/mol as well as a mean error (MAE = 0.81 kJ/mol) similar to that of the reaction energies for the same parameter setting (MAE = 0.87 kJ/mol).

Molecular Clusters and Timings. Another important group of chemical structures are clusters of small molecules. For the calculation of their binding energies, which may be based on different types of interactions (e.g., dispersion, hydrogen bonds), the choice of the basis set is very decisive. In this context, the basis set superposition error (BSSE) is a well-known problem, which results in large errors, especially when using small basis sets without a CP correction. Previously, it has been shown that the combination of the standard incremental scheme with the focal-point approach is also suitable to provide accurate binding energies in a very efficient way.[24] Nevertheless it is always useful to have another ansatz for the estimation of the CBS limit at hand, for example, the use of larger basis sets within the incremental scheme together with corresponding CBS extrapolations. Due to the domain-specific basis set approach, the common incremental scheme features an exceedingly high efficiency in this case, which is further increased by the application of PNOs in this work. Therefore, we analyzed the accuracy of our PNO-based incremental scheme with respect to our highly accurate reference for a set of 4 cluster structures[24] and took into account both the focal-point approach as well as larger target basis sets and corresponding two-point CBS(XY) extrapolations.[9,10]

DOI: 10.1021/acs.jctc.7b00654
J. Chem. Theory Comput. 2017, 13, 6023−6042

We performed calculations with the cc-pVDZ (DZ) and def2-TZVP (TZ) as well as with aVXZ′ (X = D,T,Q,5) basis sets. Here, aVXZ′ refers to combination of cc-pVXZ and aug-cc-pVXZ basis sets for different atoms according to Table 2,

Table 2. Applied aVXZ′ (X = D,T,Q,5) Basis Sets for the Test Set of Four Molecular Clusters

cluster	basis
$(H_2)_{20}$	aug-cc-pVXZ
$(CH_4)_{10}$	cc-pVXZ
$(HF)_{10}$	aug-cc-pVXZ(F)/cc-pVXZ(H)
$(H_2O)_{10}$	aug-cc-pVXZ(O)/cc-pVXZ(H)

that is, augmentation has only been used where necessary. Before considering the accuracy with respect to our highly accurate reference, we present the local errors (see Figure 15) analyzed for the smaller basis sets (DZ, TZ, aVDZ′).

The local errors are rather insensitive against the target basis set, that is, on average the MAEs are similar for TZ and aVDZ′ as well as slightly smaller for the DZ basis. As expected, the (T0) local errors are about 1 kJ/mol larger, which is due to the approximate treatment of the triples compared to the Laplace ansatz. Furthermore, the truncation parameters have a larger influence on the accuracy, as tightening from 10^{-7} to 10^{-8} reduces the MAE by around 2−4 kJ/mol. Another effect of the truncations is given by the differences between incremental and nonincremental approach. In this context, $T_{PNO} = T_{TNO} = 10^{-8}$, which refers to a well converged PNO and TNO truncation series, features only slightly worse MAEs of the conventional PNO method in comparison to the incremental ones. In contrast, with a truncation value of 10^{-7}, the MAEs of the nonincremental approach are about 1.5 kJ/mol larger. The explanation for the higher accuracy of the incremental binding energies is the MP2 correction, which mainly corrects for the incremental error but also compensates the PNO error particularly. This reduction of the PNO error has already been shown in the Error Analysis section. In order to demonstrate this behavior again, we also considered the MP2 correction for the standard PNO method. Especially for the PNO/TNO truncation with 10^{-7}, a clear decrease of the local error is recognizable, leading roughly to the accuracy of the i3-PNO approach. However, this indicates also a negligible incremental error. For $T_{PNO} = T_{TNO} = 10^{-8}$, the effect of the MP2 correction is obviously less decisive. Furthermore, the accuracy of the PNO-based incremental series is higher for a second-order truncation than for the third order, again with larger differences in case of $T_{PNO} = T_{TNO} = 10^{-7}$. It is well-known, that the third-order contribution is almost negligible for clusters consisting of small molecules, as there are no covalent interactions between the domains and the existing intermolecular forces are sufficiently described by pair interactions. In combination with PNOs, the second-order expansion seems to introduce less or smaller PNO errors with a negligible incremental error, which leads to a higher total accuracy of the local approximation. As a consequence, second-order incremental expansions of PNO−CCSD(T)/(T0) energies should be used to obtain binding energies of molecular clusters with a high accuracy and efficiency. Besides this, the accuracy with respect to the CBS limit, which is assessed in the next part, should be considered for second- and third-order expansions. After that, also the efficiency of the PNO-based incremental scheme is evaluated by means of the $(H_2O)_{10}$ and a $(H_2O)_{20}$ cluster in the last part of this section.

Regarding the accuracy relative to our reference binding energies[24] according to eq 5, the deviation between second and third incremental order is again found to be very small, as shown in Figure 16 (left) for the $(H_2O)_{10}$ cluster as well as in

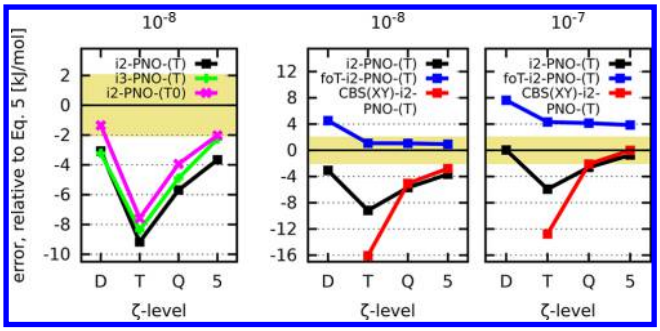


Figure 16. Convergence of the incremental PNO−CCSD(T)/(T0) binding energies errors for the $(H_2O)_{10}$ cluster relative to our reference (eq 5) with respect to the ζ-level of the applied aVXZ′ basis sets. The effects of the PNO truncation thresholds ($10^{-7}/10^{-8}$), the (T0) approximation, and the order of the incremental expansion are demonstrated. Furthermore, the accuracies of the focal-point results as well as the CBS(XY)-extrapolated energies are assessed.

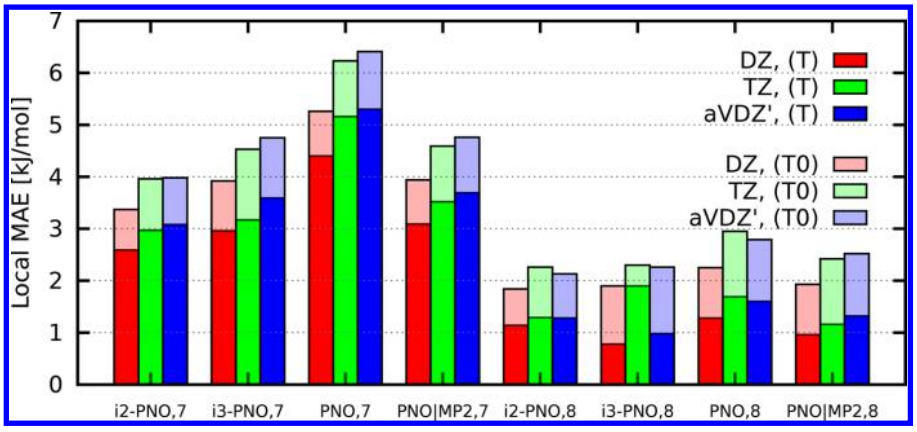


Figure 15. Local mean absolute errors (MAEs) of the second- and third-order incremental as well as the nonincremental PNO−CCSD(T) and PNO−CCSD(T0) binding energies for the cluster test set. Two different PNO/TNO truncation values, 10^{-7} (7) or 10^{-8} (8), are compared and *conv 2* was applied.

DOI: 10.1021/acs.jctc.7b00654
J. Chem. Theory Comput. 2017, 13, 6023−6042

Figure 17 (right) for the cluster test set and the combination with the focal-point approach. However, both figures also

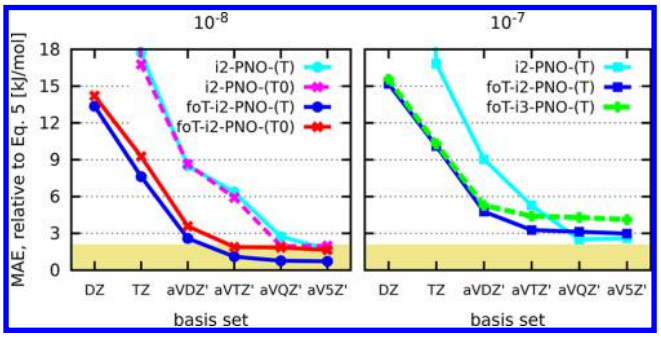


Figure 17. MAEs of the incremental PNO−CCSD(T)/(T0) binding energies errors for the 4 test set clusters relative to our reference (eq 5) for different basis sets (DZ = cc-pVDZ, TZ = def2-TZVP, aVXZ′ = (aug-)cc-pVXZ). The influences of the PNO truncation thresholds ($10^{-7}/10^{-8}$), the (T0) approximation ,and the order of the incremental expansion are demonstrated. Furthermore, the effect of the focal-point approach (foT-) on the accuracy is assessed.

indicate that this difference is increasing with the basis set size. Furthermore, the deviation depends on the system, that is, the second-order expansion is more accurate on average (Figure 17) but for the specific case of $(H_2O)_{10}$ it is slightly worse than the third order. But since a second-order truncation features clearly lower computational costs, it is used in all further considerations referring to the accuracy of the clusters binding energies.

The (T0) approximation provides an additional error, which is usually less than 1 kJ/mol on average (Figure 17, red curve) for the focal-point incremental scheme. Contrary to this, it is even slightly more accurate than the Laplace triples, considering the MAE for the pure incremental PNO method (dashed pink curve). The latter one is also recognizable for the $(H_2O)_{10}$ cluster (Figure 16, pink curve).

However, for the binding energies of the molecular clusters both discussed influences, that is, the incremental truncation order and the triples ansatz, are clearly within the chemical accuracy limit and also smaller than the effect of the PNO truncation parameters. For example, the deviations between the binding energies of $(H_2O)_{10}$ in Figure 16, obtained with $T_{PNO} = T_{TNO} = 10^{-7}$ (right) and 10^{-8} (middle), are around 3 kJ/mol, independent of the approach (pure incremental, focal-point, or two-point CBS(XY) extrapolation). Thus, also the MAE of the foT-i2-PNO−CCSD(T) method with truncation values of 10^{-7} (Figure 17, right, dark blue curve) is approximately 3 kJ/mol at the convergence limit, while the corresponding curve for $T_{PNO} = T_{TNO} = 10^{-8}$ (left, dark blue) converges clearly below 1 kJ/mol. Therefore, we recommend to use this tight truncation setting for PNOs and TNOs, if binding energies for molecular clusters shall be calculated with a high accuracy.

Finally, we also discuss the performance of the focal-point approach as well as the two-point CBS(XY) extrapolations, regarding the accuracy. When applying the recommended second-order incremental expansion and 10^{-8} for the PNO/TNO truncations, the small cc-pVDZ and def2-TZVP basis sets are not sufficient, even if the focal-point approach is used, as the remaining errors are large (see Figure 17, left). Therefore, in contrast to the reactions and intermolecular interactions, discussed in the previous sections, the focal-point approach for molecular clusters must be based on CCSD(T) calculations in larger basis sets. This is comparable to recent findings of Schmitz and Hättig.[84] Anyway, already with an aVTZ′ basis set, the foT-i2-PNO−CCSD(T) method reaches chemical accuracy for binding energies with an MAE around 1 kJ/mol and only slight changes up to the aV5Z′ basis. That way, the focal-point treatment clearly improves the results from the pure i2-PNO−CCSD(T)|MP2 calculations. With CBS(34) or CBS(45) extrapolations, the errors of the incremental binding energy from an aVQZ′ or aV5Z′ calculation is somewhat improved, when using the recommended parameter setting ($T_{PNO} = T_{TNO} = 10^{-8}$), for example, for the $(H_2O)_{10}$ cluster in Figure 16 (middle). However, even the best two-point CBS(XY) extrapolation cannot reach the accuracy of the foT-i2-PNO−CCSD(T)/aVTZ′ method and additionally needs significantly larger computation times. For the less tight truncation value (10^{-7}), CBS(34) and CBS(45) extrapolations provide some higher accuracy than the corresponding focal-point method, as demonstrated for $(H_2O)_{10}$ in Figure 16 (right) as well as for the cluster test set in Figure 18. The focal-point approach is even

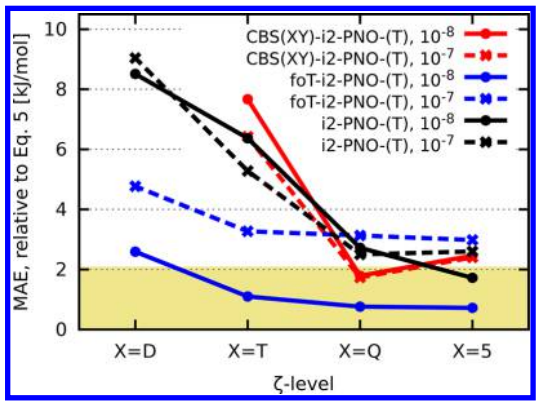


Figure 18. MAEs of the second-order incremental PNO−CCSD(T)/(T0) binding energies errors for the 4 test set clusters relative to our reference (eq 5) with respect to the ζ-level of the applied aVXZ′ basis sets for different PNO truncation thresholds ($10^{-7}/10^{-8}$). The effect of the focal-point approach (foT-) and a two-point CBS(XY) extrapolation on the accuracy is assessed.

beaten by the corresponding nonfocal incremental method. From the results for the $(H_2O)_{10}$ cluster in Figure 16 an explanation of this behavior can be derived. While the tighter truncation (10^{-8}) shows worse reduction of the basis set incompleteness error (BSIE) by two-point CBS(XY) extrapolations compared to the focal-point method, which leads to negative deviations, the looser truncation (10^{-7}) causes a positive shift of the error within the binding energy (PNO error). Thus, if $T_{PNO} = T_{TNO} = 10^{-7}$ is applied in combination with a two-point CBS(XY) extrapolation, the positive PNO error contribution and the negative one due to the larger BSIE are compensating partially. Nevertheless, at the convergence limit, the MAE of all three approaches (dashed curves in Figure 18) is similar and features an offset of scarcely 3 kJ/mol, referring to the PNO truncation error for $T_{PNO} = T_{TNO} = 10^{-7}$. Finally, after all these considerations, we evaluated the highly efficient focal-point ansatz in combination with our PNO-based incremental method as the best approach to calculate also binding energies of molecular clusters. We strongly recommend to use a tight PNO/TNO truncation threshold with a value of 10^{-8}. This is also in good agreement with the findings of Schmitz and Hättig regarding the conventional PNO binding

DOI: 10.1021/acs.jctc.7b00654
J. Chem. Theory Comput. 2017, 13, 6023−6042

energies,[84] and therefore we emphasize again that the truncation setting should be carefully selected depending on the considered system. Furthermore, at least an (aug-)cc-pVTZ basis for the CCSD(T) calculation should be chosen, while a second-order incremental expansion is clearly sufficient for these systems.

At the end of this section, we discuss the efficiency of our incremental PNO scheme in comparison to the conventional PNO method. Therefore, we analyzed the total and wall times of the $(H_2O)_{10}$ and the larger $(H_2O)_{20}$ clusters with respect to the size of the aVXZ′ basis sets.

In general, Figure 19 shows the clearly steeper increase of the computation time with respect to the ζ-level for the

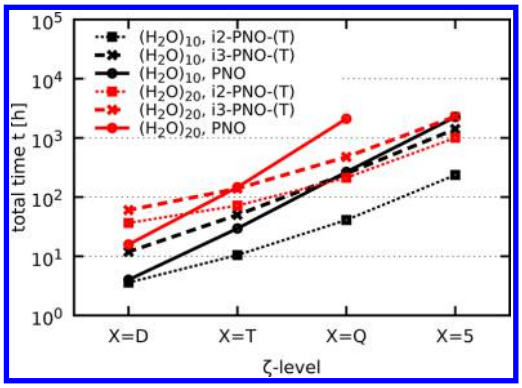


Figure 19. Total times (according to eqs 9 and 10) of the PNO-based second- (i2) and third-order (i3) incremental CCSD(T) calculations in comparison to the conventional PNO−CCSD(T) ones with respect to the ζ-level of the applied aVXZ′ basis sets for two water clusters. Furthermore, $T_{PNO} = T_{TNO} = 10^{-7}$ as well as *conv 2* were applied for the PNO scheme, and a logarithmic time-scale is used in the graph.

nonincremental PNO method. The reason is the domain-specific basis set approach within the incremental scheme, which features very high efficiencies for increasing differences of the target (here aVXZ′) and environmental (SV) basis set size in the calculation of the increments. For $T_{PNO} = T_{TNO} = 10^{-7}$ and the smaller water cluster, already with an aVDZ′ basis the recommended second-order calculation is faster than the conventional PNO, while an aVTZ′ basis is necessary for the larger cluster. However, for larger basis sets (e.g., aVQZ′), the differences in the total times are tremendous. Although a second-order truncation is appropriate for molecular clusters and their binding energies, a third-order expansion is needed for most chemical structures (i.e., covalent interactions). Therefore, we also analyzed the timings of the third-order incremental calculations. Here, the PNO calculation for the smaller cluster is slightly longer than the incremental calculation for an aVQZ′ basis, while the same holds for the larger cluster and an aVTZ′ basis. The total times for these two settings are also denoted in Table 3 and supplemented by the wall times. As a smaller basis is sufficient to obtain a faster incremental calculation for the larger system, the efficiency of the usual third-order PNO-based incremental expansion also increases with the system size. Beside the slightly smaller total times for the third order and clearly reduced ones for the second order in Table 3, especially the diminutive wall times of the incremental approach are remarkable. As the total calculation of the correlation energy is separated into several clearly smaller incremental ones, a distribution over a large number of nodes is possible, and the method is strongly

Table 3. Total Times (According to Eqs 9 and 10) and Wall Times of Selected Second- (i2) and Third-Order (i3) PNO-Based Incremental CCSD(T) Calculations in Comparison to the Conventional PNO−CCSD(T) Ones[a]

	total time [h]		wall time [h]	
	10^{-7}	10^{-8}	10^{-7}	10^{-8}
	$(H_2O)_{10}$, aVQZ′			
i2-PNO-(T)	41.0	138.8	0.33[b]	1.08[b]
i3-PNO-(T)	249.1	745.9	1.40[b]	4.61[b]
PNO-(T)	265.6	771.5	66.40	192.86
	$(H_2O)_{20}$, aVTZ′			
i2-PNO-(T)	71.8	97.6	0.35[c]	0.50[c]
i3-PNO-(T)	138.9	224.6	0.65[c]	1.11[c]
PNO-(T)	146.4	798.6	36.59	199.66

[a]An aVXZ′ basis set as well as truncation values of 10^{-7} respectively 10^{-8} and *conv 2* were applied. The total times of conventional MP2 (for MP2 correction) were added for all incremental calculations, while the corresponding wall times are only for the incremental parts (using a distribution over 1 server and 60 client nodes). [b]The wall time for the (parallel executable) MP2 calculations is 0.04 h. [c]The wall time for the (parallel executable) MP2 calculations is 0.51 h.

parallelizable. That way, we can reduce the wall time by, for example, a factor of around 50 (third order) to 100 (second order) in case of $(H_2O)_{20}$ as well as the aVTZ′ basis and obtain our results in a significantly shorter time. Furthermore, the separation into many small calculations enables the applicability to larger systems and basis sets on the same hardware, compared to the conventional PNO method, for example.

The tightening of the truncation values to 10^{-8} also influences the computation times (Figure 20), leading to an

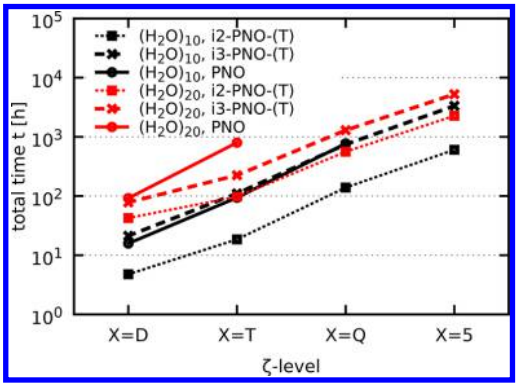


Figure 20. Total times (according to eq 9 and 10) of the PNO-based second- (i2) and third-order (i3) incremental CCSD(T) calculations in comparison to the conventional PNO−CCSD(T) ones with respect to the ζ-level of the applied aVXZ′ basis sets for two water clusters. Furthermore, $T_{PNO} = T_{TNO} = 10^{-8}$ as well as *conv 2* were applied for the PNO scheme, and a logarithmic time-scale is used in the graph.

even higher efficiency of our incremental PNO method in comparison to the conventional one, especially for the larger cluster. For the smaller cluster and an aVDZ′ basis set, the PNO calculation is clearly more demanding than the corresponding i2-PNO calculation and only slightly faster than the third-order one. Again, an aVQZ′ basis is necessary for a faster i3-PNO calculation, compared to standard PNO (see also Table 3). When increasing the system to the double-sized cluster, the total time of the conventional PNO method is now already larger than that for the third-order PNO-based

DOI: 10.1021/acs.jctc.7b00654
J. Chem. Theory Comput. 2017, 13, 6023−6042

Table 4. Binding Energies and Total Times (According to Eqs 9 and 10) of Second-Order PNO-Based Incremental CCSD(T) Calculations as Well as Resulting Focal-Point and CBS(XY)-Extrapolated Ones for $(H_2O)_{20}$[a]

	binding energy [kJ/mol]			total time [h]			
	i2-PNO	foT-i2-PNO	CBS(XY)-i2-PNO	i2-PNO	foT-i2-PNO	CBS(XY)-i2-PNO	i2
aVTZ′	−839.0	−829.4	−844.6	97.6	342.1	140.1	1431.2
aVQZ′	−829.8	−829.2	−825.4	560.6	792.6	658.2	4844.5
aV5Z′	−824.8	−829.4	−822.0	2268.7	2451.2	2829.4	
				reference binding energy from ref 84 [kJ/mol]			
fo5[b]-i2/aV5Z′				−828.4			
fo5[b]-i2/QZ-F12				−828.5			

[a]Binding energies are compared to the best available references (from ref 84) and the total times to second-order incremental calculations without PNOs. The aVXZ′ basis sets (X = T,Q,5), as well as truncation values of 10^{-8} and *conv* 2, were applied. The total times of conventional MP2 (for MP2 correction) were added for all incremental calculations. [b]Focal-point ansatz according to eq 12, using aV5Z′ instead of a XZ-F12 basis for MP2-F12.

incremental approach, using the aVDZ′ basis. As this tighter truncation setting is recommended in combination with the aVTZ′ basis, the total times for both the second and third order are clearly smaller than for the standard PNO, precisely 12% and 28% for the larger water cluster. According to Table 3, the parallelization of the incremental scheme on 60 client nodes even reduces the wall times to 0.25% (i2) and 0.56% (i3).

Finally, to show again the suitability of our recommended method, we further considered the larger $(H_2O)_{20}$ dodecahedron structure. This cluster has been focused in previous works, regarding its CBS reference binding energy.[84,145] We will demonstrate the high accuracy of our method and the tremendous efficiency in comparison to the incremental scheme without PNOs (see Table 4).

Regarding the accuracy, the nonfocal aVTZ′ calculation in Table 4 provides a large deviation. Nevertheless, with the focal-point approach the resulting binding energy agrees well with the references. An increasing of the aVXZ′ basis (i.e., to X = Q or 5) is not necessary, as the same binding energy is received. When using the two-point CBS(XY) extrapolation, the binding energies converge to a CBS(45) value with a deviation of about 5 and 8 kJ/mol from the references. Therefore, we emphasize again the suitability of the efficient focal-point scheme. The computation time of the MP2-F12/cc-pVTZ-F12 calculation of the recommended foT-i2-PNO−CCSD(T)/aVTZ′ method is clearly larger than the incremental part of the total time. However, the total time of this method is smaller than for the i2-PNO−CCSD(T)/aVQZ′ or the corresponding CBS(34)-extrapolated calculations. Furthermore, the usage of PNOs decreases the time of the MP2-corrected second-order incremental calculation to a small percentage (e.g., 6.8% for aVTZ′), compared to the common incremental scheme. That way, the tremendous enhancement of the efficiency of the incremental scheme by using PNOs is demonstrated.

Application to Large Systems. In order to show the applicability of our PNO-based incremental scheme for large systems, we performed calculations regarding the *syn*−*anti* isomerism of a double cyclohexane (*syn*-/*anti*-**2**, see top structures in Figure 21). These structures have already been considered in a work of Zhang and Dolg on the influence of dispersion on this isomerism.[173] The authors performed DFT calculations with and without dispersion correction as well as correlated calculations for smaller model adducts. Our supplemental results refer to the original structures *syn*-/*anti*-**2** as well as to Tetramethyl-substituted derivatives *syn*-**2*** and *anti*-**2*** (see bottom structures in Figure 21). The latter geometries have been optimized (according to the unsubsituted

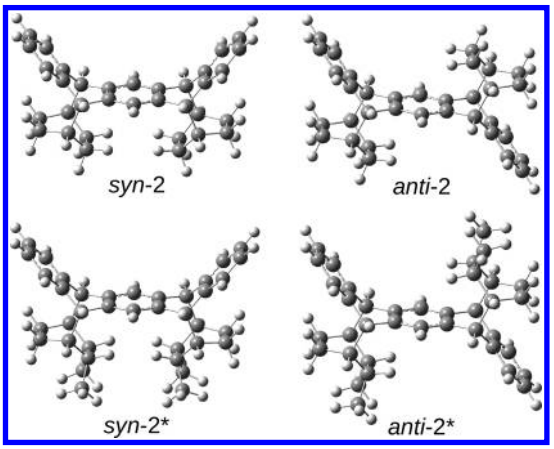


Figure 21. Structures for the application of our new method, optimized with TPSS-D3/SVP (*syn*-/*anti*-**2** from ref 173).

ones) on the TPSS-D3/SVP[158,174−176] level and characterized as minima.

Again, we applied the focal-point approach in combination with our PNO-based incremental method to approximate the CBS limit. The stability of *syn*- or *anti*-isomer is estimated by the difference of their electronic energies, that is, $\Delta E = E(syn) - E(anti)$. Our obtained results are shown in Table 5.

Zhang and Dolg found that the stability, that is, the sign of ΔE, is changed by dispersion interactions, which can be concluded from their DFT calculations for **2**. While common functionals with appropriate basis sets and Grimme's D3 dispersion correction provide a negative value, that is, the higher stability of the *syn* isomer, the neglect of dispersion changes this order. We found the same for **2***, where the introduction of the 4 methyl groups increases the dispersion contribution and leads to more negative values of ΔE, that is, a higher stabilization of the *syn* isomer. In contrast, without dispersion correction, the (positive) energy difference is also larger for **2***.

When considering the correlated methods, that is, our foT-i3-PNO approach, the influence of the PNO/TNO truncation is small, which was demonstrated for **2**. Therefore, calculations for **2*** are only performed with $T_{PNO} = T_{TNO} = 10^{-7}$. In contrast, both the small basis set (DZ/TZ) and the convergence criterion for the Laplace triples provide a larger effect on the energy difference. While enlarging the basis for PNO−CCSD(T)/(T0) to def2-TZVP decreases ΔE, tightening the threshold for the Laplace quadrature to *conv* 3 increases the value. That way, the best calculations (def2-TZVP, Laplace

DOI: 10.1021/acs.jctc.7b00654
J. Chem. Theory Comput. 2017, 13, 6023−6042

Table 5. Relative Energies, $\Delta E = E(syn) - E(anti)$ [kJ/mol], Obtained with Different DFT[174−181] and Focal-Point Third-Order Incremental PNO-Based Methods for the Structures 2 and 2*[a]

DFT Methods (ref 173 for 2)		
method	2	2*
B97-D3(BJ)/QZ	−0.4	−2.6
TPSS-D3(BJ)/QZ	−0.3	−3.0
B3LYP-D3(BJ)/TZ′	−0.3	−2.3
B97/QZ	+5.3	+9.8
TPSS/QZ	+3.5	+6.9
B3LYP/TZ′	+4.0	+8.4
foT-i3-PNO Methods		
	2	2*
method	10^{-7}	10^{-8}	10^{-7}
(T0)/DZ	+2.6	+2.3	−1.6
(T)/DZ, *conv 2*	+0.1	+0.3	−4.4
(T)/DZ, *conv 3*	+3.4	+3.1	−2.4
(T0)/TZ	+0.2	−0.3	−4.2
(T)/TZ, *conv 2*	−0.7	−0.5	
(T)/TZ, *conv 3*	+2.0	+1.1	−3.8

[a]QZVPP[182] (QZ) and TZVPP[162] (TZ′) were applied as basis sets within the DFT calculations. The incremental methods used a cc-pVDZ (DZ) or a def2-TZVP (TZ) basis set and PNO/TNO truncation thresholds of 10^{-8} (only 2) or 10^{-7} were applied.

triples with *conv 3*) yield energy differences of ΔE = +1.1 kJ/mol for 2 (with $T_{PNO} = T_{TNO} = 10^{-8}$) and ΔE = −3.8 kJ/mol for 2* (with $T_{PNO} = T_{TNO} = 10^{-7}$). Thus, for the latter one, the D3-corrected DFT and the correlated methods both feature a negative sign, that is, the higher stability of the *syn*-2* isomer by some kJ/mol. In contrast, the dispersion seems to be somewhat overestimated by the D3 correction for structure 2. In this context, the convergence criterion within the Laplace ansatz is crucial for the sign of ΔE. While the higher stability of the *anti*-2 isomer is indicated with the *conv 3* setting, the result, based on the less tight *conv 2* value, is close to the D3-corrected energy differences, which refer to a slightly higher stability of the corresponding *syn* isomer.

CONCLUSION

In this work we presented our new incremental scheme, which is based on the PNO implementation of Hättig et al., to calculate PNO−CCSD(T) and PNO−CCSD(T0) energies. Furthermore, we provided an extensive analysis of the performance of our PNO-based incremental method, regarding various types of energies, that is, reaction, intermolecular interaction, and cluster binding energies. In this context, we considered errors due to both our incremental approach and the PNO implementation. We found, that the pure incremental error is comparable for canonical and PNO methods. Therefore, a third-order expansion of PNO−CCSD(T) increments in the domain-specific basis with the well-established MP2 correction still provides very small incremental errors, which are also very insensitive against the target basis set. For clusters of small molecules, even a second-order truncation is sufficient, as known previously and confirmed in this work for the new PNO incremental scheme. Regarding the PNO error, an assessment of the accuracy with respect to the PNO and TNO truncation is essential. If the truncation parameters are tightened appropriately, the PNO error of relative energies can be reduced to very small values, and chemical accuracy can be reached by the total local errors of our PNO-based incremental scheme, when using the conventional MP2 correction to account for the domain-specific basis set approach. Similar to the recommendations for the conventional PNO method, we confirmed $T_{PNO} = T_{TNO}$ as a convenient setting. However, the optimal adjustment of these truncation parameters depends on the considered system. While 10 is usually sufficient for reaction energies, the value should be tightened to 10^{-8} for the calculation of intermolecular interactions and, especially, if binding energies of small-molecule clusters are computed.

Furthermore, we evaluated our new method in combination with the highly efficient focal-point approach to reach the CBS limit. We demonstrated by means of statistical analyses that a rather small basis set like def2-TZVP for the incremental PNO−CCSD(T) calculation and an explicitly correlated MP2 calculation with cc-pVTZ-F12 are sufficient to obtain chemical accuracy for reactions and intermolecular interactions. However, the PNO−CCSD(T) calculations of binding energies for molecular clusters within the focal-point method must be based on the larger (aug-)cc-pVTZ basis to reach this high accuracy.

For this basis, we showed that the total time of a third-order incremental expansion is lower than for the corresponding standard PNO calculation, when applied to a large cluster. However, as a second-order expansion provides a sufficient accuracy of cluster binding energies, the total time of our PNO-based scheme is further reduced to 12% of the standard PNO calculation and 7% of the corresponding conventional second-order incremental one. Thus, also the computational costs are strongly reduced with respect to the standard incremental scheme, that is, due to the introduction of PNOs. Besides this, the wall times can be decreased to a tremendously small percentage (e.g., 0.25% for $(H_2O)_{20}$), aVTZ′ and $T_{PNO} = T_{TNO} = 10^{-8}$) due to the distribution of the small, less demanding incremental computations on several client nodes. Therefore, our PNO-based incremental scheme can feature smaller total computation times in comparison to the standard PNO implementation with a high parallelizability and significantly reduced wall times as well as a very high accuracy relative to the CBS limit, reached in combination with the very efficient MP2-based focal-point approach. Due to the separation into many small calculations, larger systems in comparison to the nonincremental PNO methods are accessible.

ASSOCIATED CONTENT

Supporting Information

The Supporting Information is available free of charge on the ACS Publications website at DOI: 10.1021/acs.jctc.7b00654.

Relative energies (reactions, interactions) and absolute energies (molecular clusters with their monomers, *syn*/*anti* systems), including total energies (with HF contribution) for canonical and standard PNO methods as well as only correlation contributions for incremental PNO methods, list of reactions (FH test set) and complexes, coordinates (of complexes and *syn*-/*anti*-2*), and total times (for water clusters) (PDF)

AUTHOR INFORMATION

Corresponding Author

*E-mail: joachim.friedrich@chemie.tu-chemnitz.de.

ORCID

Benjamin Fiedler: 0000-0003-3547-0283

DOI: 10.1021/acs.jctc.7b00654
J. Chem. Theory Comput. 2017, 13, 6023−6042

Gunnar Schmitz: 0000-0003-3677-4748
Christof Hättig: 0000-0002-5752-2710

Notes

The authors declare no competing financial interest.

■ ACKNOWLEDGMENTS

B.F. and J.F. thank the DFG Research Group FOR 1497 for financial support.

■ REFERENCES

(1) Coester, F. Bound states of a many-particle system. *Nucl. Phys.* **1958**, *7*, 421−424.
(2) Coester, F.; Kümmel, H. Short-range correlations in nuclear wave functions. *Nucl. Phys.* **1960**, *17*, 477−485.
(3) Čížek, J. On the Correlation Problem in Atomic and Molecular Systems. Calculation of Wavefunction Components in Ursell-Type Expansion Using Quantum-Field Theoretical Methods. *J. Chem. Phys.* **1966**, *45*, 4256−4266.
(4) Čížek, J.; Paldus, J. Correlation problems in atomic and molecular systems III. Rederivation of the coupled-pair many-electron theory using the traditional quantum chemical methodst. *Int. J. Quantum Chem.* **1971**, *5*, 359−379.
(5) Helgaker, T.; Jørgensen, P.; Olsen, J. *Molecular Electronic-Structure Theory*; John Wiley & Sons Ltd.: Chichester, New York, Weinheim, Brisbane, Singapore, Toronto, 2012.
(6) Raghavachari, K.; Trucks, G. W.; Pople, J. A.; Head-Gordon, M. A fifth-order perturbation comparison of electron correlation theories. *Chem. Phys. Lett.* **1989**, *157*, 479−483.
(7) Stanton, J. F. Why CCSD(T) works: a different perspective. *Chem. Phys. Lett.* **1997**, *281*, 130−134.
(8) Hättig, C.; Klopper, W.; Köhn, A.; Tew, D. P. Explicitly Correlated Electrons in Molecules. *Chem. Rev.* **2012**, *112*, 4−74.
(9) Zhong, S. J.; Barnes, E. C.; Petersson, G. A. Uniformly convergent n-tuple-ζ augmented polarized (nZaP) basis sets for complete basis set extrapolations. I. Self-consistent field energies. *J. Chem. Phys.* **2008**, *129*, 184116.
(10) Halkier, A.; Helgaker, T.; Jørgensen, P.; Klopper, W.; Koch, H.; Olsen, J.; Wilson, A. K. Basis-set convergence in correlated calculations on Ne, N_2, and H_2O. *Chem. Phys. Lett.* **1998**, *286*, 243−252.
(11) Tew, D. P.; Klopper, W.; Neiss, C.; Hättig, C. Quintuple-ζ quality coupled-cluster correlation energies with triple-ζ basis sets. *Phys. Chem. Chem. Phys.* **2007**, *9*, 1921−1930.
(12) Fliegl, H.; Klopper, W. M.; Hättig, C. Coupled-cluster theory with simplified linear-r12 corrections: The CCSD(R12) model. *J. Chem. Phys.* **2005**, *122*, 084107.
(13) Hättig, C.; Tew, D. P.; Köhn, A. Accurate and efficient approximations to explicitly correlated coupled-cluster singles and doubles, CCSD-F12. *J. Chem. Phys.* **2010**, *132*, 231102.
(14) Hättig, C.; Klopper, W.; Köhn, A.; Tew, D. P. Explicitly correlated electrons in molecules. *Chem. Rev.* **2012**, *112*, 4−74.
(15) Tsuzuki, S.; Uchimaru, T.; Mikami, M.; Tanabe, K.; Sako, T.; Kuwajima, S. Molecular dynamics simulations of supercritical carbon dioxide fluid with the model potential from ab initio molecular orbital calculations. *Chem. Phys. Lett.* **1996**, *255*, 347−349.
(16) Hobza, P.; Sponer, J. Toward True DNA Base-Stacking Energies:? MP2, CCSD(T), and Complete Basis Set Calculations. *J. Am. Chem. Soc.* **2002**, *124*, 11802−11808.
(17) Jurecka, P.; Sponer, J.; Cerny, J.; Hobza, P. Benchmark database of accurate (MP2 and CCSD(T) complete basis set limit) interaction energies of small model complexes, DNA base pairs, and amino acid pairs. *Phys. Chem. Chem. Phys.* **2006**, *8*, 1985−1993.
(18) Papajak, E.; Truhlar, D. G. What are the most efficient basis set strategies for correlated wave function calculations of reaction energies and barrier heights? *J. Chem. Phys.* **2012**, *137*, 064110.
(19) Liakos, D. G.; Neese, F. Improved Correlation Energy Extrapolation Schemes Based on Local Pair Natural Orbital Methods. *J. Phys. Chem. A* **2012**, *116*, 4801−4816.
(20) Brauer, B.; Kesharwani, M. K.; Martin, J. M. L. Some observations on counterpoise corrections for explicitly correlated calculations on noncovalent interactions. *J. Chem. Theory Comput.* **2014**, *10*, 3791−3799.
(21) Marshall, M. S.; Burns, L. A.; Sherrill, C. D. Basis set convergence of the coupled-cluster correction, δ(MP2)(CCSD(T)): best practices for benchmarking non-covalent interactions and the attendant revision of the S22, NBC10, HBC6, and HSG databases. *J. Chem. Phys.* **2011**, *135*, 194102.
(22) Dunning, T. H., Jr.; Peterson, K. A. Approximating the basis set dependence of coupled cluster calculations: Evaluation of perturbation theory approximations for stable molecules. *J. Chem. Phys.* **2000**, *113*, 7799−7808.
(23) Friedrich, J. Efficient calculation of accurate reaction energies - Assessment of different models in electronic structure theory. *J. Chem. Theory Comput.* **2015**, *11*, 3596−3609.
(24) Friedrich, J.; Fiedler, B. Accurate calculation of binding energies for molecular clusters - Assessment of different models. *Chem. Phys.* **2016**, *472*, 72−80.
(25) Fedorov, D. G.; Kitaura, K. Second order Møller-Plesset perturbation theory based upon the fragment molecular orbital method. *J. Chem. Phys.* **2004**, *121*, 2483−2490.
(26) Fedorov, D. G.; Kitaura, K. Coupled-cluster theory based upon the fragment molecular-orbital method. *J. Chem. Phys.* **2005**, *123*, 134103.
(27) Fedorov, D. G.; Nagata, T.; Kitaura, K. Exploring chemistry with the fragment molecular orbital method. *Phys. Chem. Chem. Phys.* **2012**, *14*, 7562−7577.
(28) Förner, W.; Ladik, J.; Otto, P.; Cizek, J. Coupled-cluster studies. II. The role of localization in correlation calculations on extended systems. *Chem. Phys.* **1985**, *97*, 251−262.
(29) Li, S.; Shen, J.; Li, W.; Jiang, Y. An efficient implementation of the "cluster-in-molecule" approach for local electron correlation calculations. *J. Chem. Phys.* **2006**, *125*, 074109.
(30) Li, W.; Piecuch, P.; Gour, J. R.; Li, S. Local correlation calculations using standard and renormalized coupled-cluster approaches. *J. Chem. Phys.* **2009**, *131*, 114109.
(31) Li, W.; Piecuch, P. Multilevel Extension of the Cluster-in-Molecule Local Correlation Methodology: Merging Coupled-Cluster and Mller-Plesset Perturbation Theories. *J. Phys. Chem. A* **2010**, *114*, 6721−6727.
(32) Li, W.; Guo, Y.; Li, S. A refined cluster-in-molecule local correlation approach for predicting the relative energies of large systems. *Phys. Chem. Chem. Phys.* **2012**, *14*, 7854−7862.
(33) Rolik, Z.; Kállay, M. A general-order local coupled-cluster method based on the cluster-in-molecule approach. *J. Chem. Phys.* **2011**, *135*, 104111.
(34) Rolik, Z.; Szegedy, L.; Ladjánszki, I.; Ladóczki, B.; Kállay, M. An efficient linear-scaling CCSD(T) method based on local natural orbitals. *J. Chem. Phys.* **2013**, *139*, 094105.
(35) Ziółkowski, M.; Jansík, B.; Kjærgaard, T.; Jørgensen, P. Linear scaling coupled cluster method with correlation energy based error control. *J. Chem. Phys.* **2010**, *133*, 014107.
(36) Kristensen, K.; Ziółkowski, M.; Jansík, B.; Kjærgaard, T.; Jørgensen, P. A Locality Analysis of the Divide-Expand-Consolidate Coupled Cluster Amplitude Equations. *J. Chem. Theory Comput.* **2011**, *7*, 1677−1694.
(37) Høyvik, I.-M.; Kristensen, K.; Jansík, B.; Jørgensen, P. The divide-expand-consolidate family of coupled cluster methods: numerical illustrations using second order Møller-Plesset perturbation theory. *J. Chem. Phys.* **2012**, *136*, 014105.
(38) Flocke, N.; Bartlett, R. J. A natural linear scaling coupled-cluster method. *J. Chem. Phys.* **2004**, *121*, 10935−10944.
(39) Hughes, T. F.; Flocke, N.; Bartlett, R. J. Natural Linear-Scaled Coupled-Cluster Theory with Local Transferable Triple Excitations: Applications to Peptides. *J. Phys. Chem. A* **2008**, *112*, 5994−6003.
(40) Hughes, T. F.; Bartlett, R. J. Transferability in the natural linear-scaled coupled-cluster effective Hamiltonian approach: Applications to

DOI: 10.1021/acs.jctc.7b00654
J. Chem. Theory Comput. 2017, 13, 6023−6042

dynamic polarizabilities and dispersion coefficients. *J. Chem. Phys.* **2008**, *129*, 054105.
(41) Yang, W. Direct calculation of electron density in density-functional theory. *Phys. Rev. Lett.* **1991**, *66*, 1438−1441.
(42) Kobayashi, M.; Nakai, H. Divide-and-conquer-based linear-scaling approach for traditional and renormalized coupled cluster methods with single, double, and noniterative triple excitations. *J. Chem. Phys.* **2009**, *131*, 114108.
(43) Kobayashi, M.; Nakai, H. How does it become possible to treat delocalized and/or open-shell systems in fragmentation-based linear-scaling electronic structure calculations? The case of the divide-and-conquer method. *Phys. Chem. Chem. Phys.* **2012**, *14*, 7629−7639.
(44) Qi, H. W.; Leverentz, H. R.; Truhlar, D. G. Water 16-mers and Hexamers: Assessment of the Three-Body and Electrostatically Embedded Many-Body Approximations of the Correlation Energy or the Nonlocal Energy As Ways to Include Cooperative Effects. *J. Phys. Chem. A* **2013**, *117*, 4486−4499.
(45) Pulay, P. Localizability of dynamic electron correlation. *Chem. Phys. Lett.* **1983**, *100*, 151−154.
(46) Saebø, S.; Pulay, P. Local configuration interaction: An efficient approach for larger molecules. *Chem. Phys. Lett.* **1985**, *113*, 13−18.
(47) Pulay, P.; Saebø, S. Orbital-invariant formulation and second-order gradient evaluation in Mller-Plesset perturbation theory. *Theor. Chim. Acta* **1986**, *69*, 357−368.
(48) Saebø, S.; Pulay, P. Fourth-order Møller-Plesset perturbation theory in the local correlation treatment. I. Method. *J. Chem. Phys.* **1987**, *86*, 914−922.
(49) Saebø, S.; Pulay, P. Local Treatment of Electron Correlation. *Annu. Rev. Phys. Chem.* **1993**, *44*, 213−236.
(50) Hampel, C.; Werner, H.-J. Local treatment of electron correlation in coupled cluster theory. *J. Chem. Phys.* **1996**, *104*, 6286−6297.
(51) Schütz, M.; Hetzer, G.; Werner, H.-J. Low-order scaling local electron correlation methods. I. Linear scaling local MP2. *J. Chem. Phys.* **1999**, *111*, 5691−5705.
(52) Schütz, M. Low-order scaling local electron correlation methods. III. Linear scaling local perturbative triples correction (T). *J. Chem. Phys.* **2000**, *113*, 9986−10001.
(53) Schütz, M.; Werner, H.-J. Low-order scaling local electron correlation methods. IV. Linear scaling local coupled-cluster (LCCSD). *J. Chem. Phys.* **2001**, *114*, 661−681.
(54) Werner, H.-J. Eliminating the domain error in local explicitly correlated second-order Møller-Plesset perturbation theory. *J. Chem. Phys.* **2008**, *129*, 101103.
(55) Adler, T. B.; Werner, H.-J. Local explicitly correlated coupled-cluster methods: Efficient removal of the basis set incompleteness and domain errors. *J. Chem. Phys.* **2009**, *130*, 241101.
(56) Werner, H.-J.; Schütz, M. An efficient local coupled cluster method for accurate thermochemistry of large systems. *J. Chem. Phys.* **2011**, *135*, 144116.
(57) Adler, T. B.; Werner, H.-J. An explicitly correlated local coupled cluster method for calculations of large molecules close to the basis set limit. *J. Chem. Phys.* **2011**, *135*, 144117.
(58) Scuseria, G. E.; Ayala, P. Y. Linear scaling coupled cluster and perturbation theories in the atomic orbital basis. *J. Chem. Phys.* **1999**, *111*, 8330−8343.
(59) Subotnik, J. E.; Head-Gordon, M. A local correlation model that yields intrinsically smooth potential-energy surfaces. *J. Chem. Phys.* **2005**, *123*, 064108.
(60) Subotnik, J. E.; Sodt, A.; Head-Gordon, M. A near linear-scaling smooth local coupled cluster algorithm for electronic structure. *J. Chem. Phys.* **2006**, *125*, 074116.
(61) Neese, F.; Wennmohs, F.; Hansen, A. Efficient and accurate local approximations to coupled-electron pair approaches: An attempt to revive the pair natural orbital method. *J. Chem. Phys.* **2009**, *130*, 114108.
(62) Neese, F.; Hansen, A.; Liakos, D. G. Efficient and accurate approximations to the local coupled cluster singles doubles method using a truncated pair natural orbital basis. *J. Chem. Phys.* **2009**, *131*, 064103.
(63) Liakos, D. G.; Hansen, A.; Neese, F. Weak Molecular Interactions Studied with Parallel Implementations of the Local Pair Natural Orbital Coupled Pair and Coupled Cluster Methods. *J. Chem. Theory Comput.* **2011**, *7*, 76−87.
(64) Hansen, A.; Liakos, D. G.; Neese, F. Efficient and accurate local single reference correlation methods for high-spin open-shell molecules using pair natural orbitals. *J. Chem. Phys.* **2011**, *135*, 214102.
(65) Liakos, D. G.; Neese, F. Improved correlation energy extrapolation schemes based on local pair natural orbital methods. *J. Phys. Chem. A* **2012**, *116*, 4801−4816.
(66) Riplinger, C.; Neese, F. An efficient and near linear scaling pair natural orbital based local coupled cluster method. *J. Chem. Phys.* **2013**, *138*, 034106.
(67) Riplinger, C.; Sandhoefer, B.; Hansen, A.; Neese, F. Natural triple excitations in local coupled cluster calculations with pair natural orbitals. *J. Chem. Phys.* **2013**, *139*, 134101.
(68) Pavosevic, F.; Neese, F.; Valeev, E. F. Geminal-spanning orbitals make explicitly correlated reduced-scaling coupled-cluster methods robust, yet simple. *J. Chem. Phys.* **2014**, *141*, 054106.
(69) Liakos, D. G.; Sparta, M.; Kesharwani, M. K.; Martin, J. M. L.; Neese, F. Exploring the Accuracy Limits of Local Pair Natural Orbital Coupled-Cluster Theory. *J. Chem. Theory Comput.* **2015**, *11*, 1525−1539.
(70) Liakos, D. G.; Neese, F. Is It Possible To Obtain Coupled Cluster Quality Energies at near Density Functional Theory Cost? Domain-Based Local Pair Natural Orbital Coupled Cluster vs Modern Density Functional Theory. *J. Chem. Theory Comput.* **2015**, *11*, 4054−4063.
(71) Krause, C.; Werner, H.-J. Comparison of explicitly correlated local coupled-cluster methods with various choices of virtual orbitals. *Phys. Chem. Chem. Phys.* **2012**, *14*, 7591−7604.
(72) Werner, H.-J.; Knizia, G.; Krause, C.; Schwilk, M.; Dornbach, M. Scalable electron correlation methods I.: PNO-LMP2 with linear scaling in the molecular size and near-inverse-linear scaling in the number of processors. *J. Chem. Theory Comput.* **2015**, *11*, 484−507.
(73) Ma, Q.; Werner, H.-J. Scalable Electron Correlation Methods. 2. Parallel PNO-LMP2-F12 with Near Linear Scaling in the Molecular Size. *J. Chem. Theory Comput.* **2015**, *11*, 5291−5304.
(74) Tew, D. P.; Helmich, B.; Hättig, C. Local explicitly correlated second-order Møller-Plesset perturbation theory with pair natural orbitals. *J. Chem. Phys.* **2011**, *135*, 074107.
(75) Helmich, B.; Hättig, C. Local pair natural orbitals for excited states. *J. Chem. Phys.* **2011**, *135*, 214106.
(76) Hättig, C.; Tew, D. P.; Helmich, B. Local explicitly correlated second- and third-order Møller-Plesset perturbation theory with pair natural orbitals. *J. Chem. Phys.* **2012**, *136*, 204105.
(77) Tew, D. P.; Hättig, C. Pair natural orbitals in explicitly correlated second-order møller-plesset theory. *Int. J. Quantum Chem.* **2013**, *113*, 224−229.
(78) Helmich, B.; Hättig, C. A pair natural orbital implementation of the coupled cluster model CC2 for excitation energies. *J. Chem. Phys.* **2013**, *139*, 084114.
(79) Schmitz, G.; Helmich, B.; Hättig, C. A $O(N)^3$ scaling PNO-MP2 method using a hybrid OSV-PNO approach with an iterative direct generation of OSVs. *Mol. Phys.* **2013**, *111*, 2463−2476.
(80) Helmich, B.; Hättig, C. A pair natural orbital based implementation of ADC(2)-x: Perspectives and challenges for response methods for singly and doubly excited states in large molecules. *Comput. Theor. Chem.* **2014**, *1040−1041*, 35−44.
(81) Schmitz, G.; Hättig, C.; Tew, D. P. Explicitly correlated PNO-MP2 and PNO-CCSD and their application to the S66 set and large molecular systems. *Phys. Chem. Chem. Phys.* **2014**, *16*, 22167−22178.
(82) Schmitz, G.; Hättig, C. Perturbative triples correction for local pair natural orbital based explicitly correlated CCSD(F12*) using Laplace transformation techniques. *J. Chem. Phys.* **2016**, *145*, 234107.

DOI: 10.1021/acs.jctc.7b00654
J. Chem. Theory Comput. 2017, 13, 6023−6042

(83) Frank, M. S.; Schmitz, G.; Hättig, C. The PNO-MP2 gradient and its application to molecular geometry optimizations. *Mol. Phys.* **2017**, *115*, 343−356.
(84) Schmitz, G.; Hättig, C. Accuracy of explicitly correlated local PNO-CCSD(T). *J. Chem. Theory Comput.* **2017**, *13*, 2623.
(85) Stoll, H. The correlation energy of crystalline silicon. *Chem. Phys. Lett.* **1992**, *191*, 548−552.
(86) Stoll, H. Correlation energy of diamond. *Phys. Rev. B: Condens. Matter Mater. Phys.* **1992**, *46*, 6700−6704.
(87) Stoll, H. On the correlation energy of graphite. *J. Chem. Phys.* **1992**, *97*, 8449−8454.
(88) Nesbet, R. K. Atomic Bethe-Goldstone Equations. *Phys. Rev.* **1967**, *155*, 51−55.
(89) Nesbet, R. K. Atomic Bethe-Goldstone Equations. III. Correlation Energies of Ground States of Be, B, C, N, O, F, and Ne. *Phys. Rev.* **1968**, *175*, 2−9.
(90) Nesbet, R. K. Atomic Bethe-Goldstone equations. *Adv. Chem. Phys.* **1969**, *14*, 1−34.
(91) Doll, K.; Dolg, M.; Fulde, P.; Stoll, H. Correlation effects in ionic crystals: The cohesive energy of MgO. *Phys. Rev. B: Condens. Matter Mater. Phys.* **1995**, *52*, 4842−4848.
(92) Doll, K.; Dolg, M.; Stoll, H. Correlation effects in MgO and CaO: Cohesive energies and lattice constants. *Phys. Rev. B: Condens. Matter Mater. Phys.* **1996**, *54*, 13529−13534.
(93) Doll, K.; Dolg, M.; Fulde, P.; Stoll, H. Quantum chemical approach to cohesive properties of NiO. *Phys. Rev. B: Condens. Matter Mater. Phys.* **1997**, *55*, 10282−10287.
(94) Kalvoda, S.; Dolg, M.; Flad, H.-J.; Fulde, P.; Stoll, H. Ab initio approach to cohesive properties of GdN. *Phys. Rev. B: Condens. Matter Mater. Phys.* **1998**, *57*, 2127−2133.
(95) Rosciszewski, K.; Paulus, B.; Fulde, P.; Stoll, H. Ab initio calculation of ground-state properties of rare-gas crystals. *Phys. Rev. B: Condens. Matter Mater. Phys.* **1999**, *60*, 7905−7910.
(96) Rosciszewski, K.; Paulus, B.; Fulde, P.; Stoll, H. Ab initio coupled-cluster calculations for the fcc and hcp structures of rare-gas solids. *Phys. Rev. B: Condens. Matter Mater. Phys.* **2000**, *62*, 5482−5488.
(97) Stoll, H.; Paulus, B.; Fulde, P. On the accuracy of correlation-energy expansions in terms of local increments. *J. Chem. Phys.* **2005**, *123*, 144108.
(98) Müller, C.; Herschend, B.; Hermansson, K.; Paulus, B. Application of the method of increments to the adsorption of CO on the CeO_2 (110) surface. *J. Chem. Phys.* **2008**, *128*, 214701.
(99) Schmitt, I.; Fink, K.; Staemmler, V. The method of local increments for the calculation of adsorption energies of atoms and small molecules on solid surfaces Part I. A single Cu atom on the polar surfaces of ZnO. *Phys. Chem. Chem. Phys.* **2009**, *11*, 11196−11206.
(100) Müller, C.; Hermansson, K.; Paulus, B. Electron correlation contribution to the N_2O/ceria(111) interaction. *Chem. Phys.* **2009**, *362*, 91−96.
(101) Staemmler, V. Method of Local Increments for the Calculation of Adsorption Energies of Atoms and Small Molecules on Solid Surfaces. 2. CO/MgO(001). *J. Phys. Chem. A* **2011**, *115*, 7153−7160.
(102) Müller, C.; Usvyat, D. *J. Chem. Theory Comput.* **2013**, *9*, 5590−5598.
(103) Stoll, H.; Doll, K. Approaching the bulk limit with finite cluster calculations using local increments: The case of LiH. *J. Chem. Phys.* **2012**, *136*, 074106.
(104) de Lara-Castells, M. P.; Stoll, H.; Mitrushchenkov, A. O. Assessing the Performance of Dispersionless and Dispersion-Accounting Methods: Helium Interaction with Cluster Models of the TiO_2(110) Surface. *J. Phys. Chem. A* **2014**, *118*, 6367−6384.
(105) de Lara-Castells, M. P.; Bartolomei, M.; Mitrushchenkov, A. O.; Stoll, H. Transferability and accuracy by combining dispersionless density functional and incremental post-Hartree-Fock theories: Noble gases adsorption on coronene/graphene/graphite surfaces. *J. Chem. Phys.* **2015**, *143*, 194701.
(106) Kalvoda, S.; Paulus, B.; Dolg, M.; Stoll, H.; Werner, H.-J. Electron correlation effects on structural and cohesive properties of closo-hydroborate dianions $(B_nH_n)^{2-}$ (n= 5−12) and B_4H_4. *Phys. Chem. Chem. Phys.* **2001**, *3*, 514−522.
(107) Paulus, B. Wave-function-based ab initio correlation treatment for the buckminsterfullerene C_{60}. *Int. J. Quantum Chem.* **2004**, *100*, 1026−1032.
(108) Friedrich, J.; Perlt, E.; Roatsch, M.; Spickermann, C.; Kirchner, B. Coupled cluster in condensed phase. Part I. Static quantum chemical calculations of hydrogen fluoride clusters. *J. Chem. Theory Comput.* **2011**, *7*, 843−851.
(109) Spickermann, C.; Perlt, E.; Domaros, M.; Roatsch, M.; Friedrich, J.; Kirchner, B. Coupled Cluster in Condensed Phase. Part II: Liquid Hydrogen Fluoride from Quantum Cluster Equilibrium Theory. *J. Chem. Theory Comput.* **2011**, *7*, 868−875.
(110) Perlt, E.; Friedrich, J.; Domaros, M.; Kirchner, B. Importance of structural motifs in liquid hydrogen fluoride. *ChemPhysChem* **2011**, *12*, 3474−3482.
(111) Polenz, I.; Schmidt, F. G.; Friedrich, J.; Tchernook, I.; Spange, S. Radical Polymerization of MMA co-initiated by 2-Phenyloxazoline. *Macromol. Chem. Phys.* **2013**, *214*, 1473−1483.
(112) Zhang, J.; Dolg, M. Third-Order Incremental Dual-Basis Set Zero-Buffer Approach: An Accurate and Efficient Way To Obtain CCSD and CCSD(T) Energies. *J. Chem. Theory Comput.* **2013**, *9*, 2992−3003.
(113) Zhang, J.; Heinz, N.; Dolg, M. Understanding lanthanoid(III) hydration structure and kinetics by insights from energies and wave functions. *Inorg. Chem.* **2014**, *53*, 7700−7708.
(114) Mata, R. A.; Stoll, H. An incremental correlation approach to excited state energies based on natural transition/localized orbitals. *J. Chem. Phys.* **2011**, *134*, 034122.
(115) Zhang, J.; Dolg, M. Approaching the complete basis set limit of CCSD(T) for large systems by the third-order incremental dual-basis set zero-buffer F12 method. *J. Chem. Phys.* **2014**, *140*, 044114.
(116) Mödll, M.; Dolg, M.; Fulde, P.; Stoll, H. Quantum chemical ab initio calculations of the magnetic interaction in alkalithioferrates(III). *J. Chem. Phys.* **1997**, *106*, 1836−1846.
(117) Friedrich, J.; Hanrath, M.; Dolg, M. Evaluation of incremental correlation energies for open-shell systems: Application to the intermediates of the 4-exo cyclization, Arduengo carbenes and an anionic water cluster. *J. Phys. Chem. A* **2008**, *112*, 8762−8766.
(118) Zhang, J.; Dolg, M. Third-Order Incremental Dual-Basis Set Zero-Buffer Approach for Large High-Spin Open-Shell Systems. *J. Chem. Theory Comput.* **2015**, *11*, 962−968.
(119) Anacker, T.; Tew, D. P.; Friedrich, J. First UHF Implementation of the Incremental Scheme for Open-Shell Systems. *J. Chem. Theory Comput.* **2016**, *12*, 65−78.
(120) Fiedler, B.; Coriani, S.; Friedrich, J. Molecular Dipole Moments within the Incremental Scheme using the Domain-Specific Basis-Set Approach. *J. Chem. Theory Comput.* **2016**, *12*, 3040−3052.
(121) Friedrich, J.; Coriani, S.; Helgaker, T.; Dolg, M. Implementation of the Incremental Scheme for One-Electron First-Order Properties in Coupled-Cluster Theory. *J. Chem. Phys.* **2009**, *131*, 154102.
(122) Yang, J.; Dolg, M. Evaluation of electronic correlation contributions for optical tensors of large systems using the incremental scheme. *J. Chem. Phys.* **2007**, *127*, 084108.
(123) Friedrich, J.; McAlexander, H.; Kumar, A.; Crawford, T. D. Incremental evaluation of coupled cluster dipole polarizabilities. *Phys. Chem. Chem. Phys.* **2015**, *17*, 14284−14296.
(124) Friedrich, J.; Hanrath, M.; Dolg, M. Fully automated implementation of the incremental scheme: Application to CCSD energies for hydrocarbons and transition metal compounds. *J. Chem. Phys.* **2007**, *126*, 154110.
(125) Friedrich, J.; Hanrath, M.; Dolg, M. Error analysis of incremental electron correlation calculations and applications to clusters and potential energy surfaces. *Chem. Phys.* **2007**, *338*, 33−43.
(126) Friedrich, J.; Hanrath, M.; Dolg, M. Energy screening for the incremental scheme: Application to intermolecular interactions. *J. Phys. Chem. A* **2007**, *111*, 9830−9837.

DOI: 10.1021/acs.jctc.7b00654
J. Chem. Theory Comput. 2017, 13, 6023−6042

(127) Foster, J. M.; Boys, S. F. Canonical Configurational Interaction Procedure. *Rev. Mod. Phys.* **1960**, *32*, 300−302.
(128) Friedrich, J.; Hänchen, J. Incremental CCSD(T)(F12*)|MP2-A black box method to obtain highly accurate reaction energies. *J. Chem. Theory Comput.* **2013**, *9*, 5381−5394.
(129) Friedrich, J.; Dolg, M. Implementation and performance of a domain-specific basis set incremental approach for correlation energies: Applications to hydrocarbons and a glycine oligomer. *J. Chem. Phys.* **2008**, *129*, 244105.
(130) Friedrich, J. Localized Orbitals for Incremental Evaluations of the Correlation Energy within the Domain-Specific Basis Set Approach. *J. Chem. Theory Comput.* **2010**, *6*, 1834−1842.
(131) Fiedler, B.; Himmel, D.; Krossing, I.; Friedrich, J. A New Local Focal-Point Method - Assessment and Application to the Intramolecular Decomposition of Tris-perfluoro-tert-butoxyalane. *J. Chem. Theory Comput.* **2017**, manuscript in preparation.
(132) Friedrich, J. Incremental Scheme for Intermolecular Interactions: Benchmarking the Accuracy and the Efficiency. *J. Chem. Theory Comput.* **2012**, *8*, 1597−1607.
(133) Friedrich, J.; Walczak, K. Incremental CCSD(T)(F12)|MP2-F12-A method to obtain highly accurate CCSD(T) energies for large molecules. *J. Chem. Theory Comput.* **2013**, *9*, 408−417.
(134) Edmiston, C.; Krauss, M. Configuration-Interaction Calculation of H_3 and H_2. *J. Chem. Phys.* **1965**, *42*, 1119−1120.
(135) Edmiston, C.; Krauss, M. Pseudonatural Orbitals as a Basis for the Superposition of Configurations. I. He^{2+}. *J. Chem. Phys.* **1966**, *45*, 1833−1839.
(136) Meyer, W. Ionization energies of water from PNO-CI calculations. *Int. J. Quantum Chem.* **1971**, *5*, 341−348.
(137) Meyer, W. PNO-CI Studies of electron correlation effects. I. Configuration expansion by means of nonorthogonal orbitals, and application to the ground state and ionized states of methane. *J. Chem. Phys.* **1973**, *58*, 1017−1035.
(138) Meyer, W. PNO-CI and CEPA studies of electron correlation effects. *Theor. Chim. Acta* **1974**, *35*, 277−292.
(139) Ahlrichs, R.; Lischka, H.; Staemmler, V.; Kutzelnigg, W. PNO-CI (Pair Natural Orbital Configuration Interaction) and CEPA-PNO (Coupled Electron Pair Approximation with Pair Natural Orbitals) Calculations of Molecular Systems. I. Outline of the Method for Closed-Shell States. *J. Chem. Phys.* **1975**, *62*, 1225.
(140) Ahlrichs, R.; Driessler, F.; Lischka, H.; Staemmler, V.; Kutzelnigg, W. PNO-CI (Pair Natural Orbital Configuration Interaction) and CEPA-PNO (Coupled Electron Pair Approximation with Pair Natural Orbitals) Calculations of Molecular Systems. II. The Molecules BeH_2, BH, BH_3, CH_4, CH_3−, NH_3 (Planar and Pyramidal), H_2O, OH_3+, HF and the Ne Atom. *J. Chem. Phys.* **1975**, *62*, 1235.
(141) Ahlrichs, R.; Keil, F.; Lischka, H.; Kutzelnigg, W.; Staemmler, V. PNO-CI (Pair Natural-Orbital Configuration Interaction) and CEPA-PNO (Coupled Electron Pair Approximation with Pair Natural Orbitals) Calculations of Molecular Systems. III. The Molecules MgH_2, AlH_3, SiH_4, PH_3 (Planar and Pyramidal), H_2S, HCl, and the Ar Atom. *J. Chem. Phys.* **1975**, *63*, 455.
(142) Yang, J.; Kurashige, Y.; Manby, F. R.; Chan, G. K. L. Tensor factorizations of local second-order Møller-Plesset theory. *J. Chem. Phys.* **2011**, *134*, 044123.
(143) Yang, J.; Chan, G. K.-L.; Manby, F. R.; Schütz, M.; Werner, H.-J. The orbital-specific-virtual local coupled cluster singles and doubles method. *J. Chem. Phys.* **2012**, *136*, 144105.
(144) Friedrich, J. Efficient calculation of accurate reaction energies - Assessment of different models in electronic structure theory. *J. Chem. Theory Comput.* **2015**, *11*, 3596−3609.
(145) Anacker, T.; Friedrich, J. New Accurate Benchmark Energies for Large Water Clusters − DFT is Better Than Expected. *J. Comput. Chem.* **2014**, *35*, 634−643.
(146) Köhn, A. Explicitly correlated coupled-cluster theory using cusp conditions. II. Treatment of connected triple excitations. *J. Chem. Phys.* **2010**, *133*, 174118.
(147) Hill, J. G.; Peterson, K. A.; Knizia, G.; Werner, H.-J. Extrapolating MP2 and CCSD explicitly correlated correlation energies to the complete basis set limit with first and second row correlation consistent basis sets. *J. Chem. Phys.* **2009**, *131*, 194105.
(148) Császár, A. G.; Allen, W. D.; Schaefer, H. F., III In pursuit of the ab initio limit for conformational energy prototypes. *J. Chem. Phys.* **1998**, *108*, 9751−9764.
(149) Császár, A. G.; Leininger, M. L.; Szalay, V. The standard enthalpy of formation of CH_2. *J. Chem. Phys.* **2003**, *118*, 10631−10642.
(150) Balabin, R. M. Tautomeric equilibrium and hydrogen shifts in tetrazole and triazoles: Focal-point analysis and ab initio limit. *J. Chem. Phys.* **2009**, *131*, 154307.
(151) Balabin, R. M. Conformational equilibrium in glycine: Focal-point analysis and ab initio limit. *Chem. Phys. Lett.* **2009**, *479*, 195−200.
(152) Balabin, R. M. Conformational equilibrium in alanine: Focal-point analysis and ab initio limit. *Comput. Theor. Chem.* **2011**, *965*, 15−21.
(153) Schuurman, M. S.; Muir, S. R.; Allen, W. D.; Schaefer, H. F., III Toward subchemical accuracy in computational thermochemistry: focal point analysis of the heat of formation of NCO and [H, N,C,O] isomers. *J. Chem. Phys.* **2004**, *120*, 11586−11599.
(154) Bachorz, R. A.; Bischoff, F. A.; Glöß, A.; Hättig, C.; Höfener, S.; Klopper, W.; Tew, D. P. The MP2-F12 method in the TURBOMOLE program package. *J. Comput. Chem.* **2011**, *32*, 2492−2513.
(155) TURBOMOLE development version. 2009; For further information, see http://www.turbomole.com.
(156) Ahlrichs, R.; Bär, M.; Häser, M.; Horn, H.; Kölmel, C. Electronic Structure Calculations on Workstation Computers - The Program System Turbomole. *Chem. Phys. Lett.* **1989**, *162*, 165−169.
(157) Friedrich, J.; Tew, D. P.; Klopper, W.; Dolg, M. Automated incremental scheme for explicitly correlated methods. *J. Chem. Phys.* **2010**, *132*, 164114.
(158) Schäfer, A.; Horn, H.; Ahlrichs, R. Fully optimized contracted Gaussian basis sets for atoms Li to Kr. *J. Chem. Phys.* **1992**, *97*, 2571−2577.
(159) Dunning, T. H., Jr. Gaussian basis sets for use in correlated molecular calculations. I. The atoms boron through neon and hydrogen. *J. Chem. Phys.* **1989**, *90*, 1007−1023.
(160) Woon, D.; Dunning, T. H., Jr. Gaussian basis sets for use in correlated molecular calculations. III. The atoms aluminum through argon. *J. Chem. Phys.* **1993**, *98*, 1358−1371.
(161) Kendall, R. A.; Dunning, T. H.; Harrison, R. J. Electron affinities of the first-row atoms revisited. Systematic basis sets and wave functions. *J. Chem. Phys.* **1992**, *96*, 6796−6806.
(162) Weigend, F.; Häser, M.; Patzelt, H.; Ahlrichs, R. RI-MP2: optimized auxiliary basis sets and demonstration of efficiency. *Chem. Phys. Lett.* **1998**, *294*, 143−152.
(163) Weigend, F.; Ahlrichs, R. Balanced basis sets of split valence, triple zeta valence and quadruple zeta valence quality for H to Rn: Design and assessment of accuracy. *Phys. Chem. Chem. Phys.* **2005**, *7*, 3297−3305.
(164) Peterson, K. A.; Adler, T. B.; Werner, H.-J. Systematically convergent basis sets for explicitly correlated wavefunctions: The atoms H, He, B-Ne, and Al-Ar. *J. Chem. Phys.* **2008**, *128*, 084102.
(165) Hill, J. G.; Mazumder, S.; Peterson, K. CV basis sets for explicitly correlated wavefunctions (cc-pCVnZ-F12): B-Ne and Al-Ar. *J. Chem. Phys.* **2010**, *132*, 054108.
(166) Yousaf, K. E.; Peterson, K. Optimized auxiliary basis sets for explicitly correlated methods. *J. Chem. Phys.* **2008**, *129*, 184108.
(167) Ten-no, S. Initiation of explicitly correlated Slater-type geminal theory. *Chem. Phys. Lett.* **2004**, *398*, 56−61.
(168) Tew, D. P.; Klopper, W. New correlation factors for explicitly correlated electronic wave functions. *J. Chem. Phys.* **2005**, *123*, 074101.
(169) Klopper, W.; Samson, C. C. M. Explicitly correlated second-order Møller−Plesset methods with auxiliary basis sets. *J. Chem. Phys.* **2002**, *116*, 6397−6410.

DOI: 10.1021/acs.jctc.7b00654
J. Chem. Theory Comput. 2017, 13, 6023−6042

(170) Ten-no, S. Explicitly correlated second order perturbation theory: Introduction of a rational generator and numerical quadratures. *J. Chem. Phys.* **2004**, *121*, 117−129.
(171) Knizia, G.; Werner, H.-J. Explicitly correlated RMP2 for high-spin open-shell reference states. *J. Chem. Phys.* **2008**, *128*, 154103.
(172) Knizia, G.; Adler, T. B.; Werner, H.-J. Simplified CCSD(T)-F12 methods: theory and benchmarks. *J. Chem. Phys.* **2009**, *130*, 054104.
(173) Zhang, J.; Dolg, M. Dispersion Interaction Stabilizes Sterically Hindered Double Fullerenes. *Chem. - Eur. J.* **2014**, *20*, 13909−13912.
(174) Perdew, J. P.; Wang, Y. Accurate and simple analytic representation of the electron-gas correlation energy. *Phys. Rev. B: Condens. Matter Mater. Phys.* **1992**, *45*, 13244−13249.
(175) Tao, J.; Perdew, J. P.; Staroverov, V. N.; Scuseria, G. E. Climbing the density functional ladder: nonempirical meta-generalized gradient approximation designed for molecules and solids. *Phys. Rev. Lett.* **2003**, *91*, 146401.
(176) Grimme, S.; Antony, J.; Ehrlich, S.; Krieg, H. A consistent and accurate ab initio parametrization of density functional dispersion correction (DFT-D) for the 94 elements H-Pu. *J. Chem. Phys.* **2010**, *132*, 154104.
(177) Grimme, S. Semiempirical GGA-type density functional constructed with a long-range dispersion correction. *J. Comput. Chem.* **2006**, *27*, 1787−1799.
(178) Lee, C.; Yang, W.; Parr, R. G. Development of the Colle-Salvetti correlation-energy formula into a functional of the electron density. *Phys. Rev. B: Condens. Matter Mater. Phys.* **1988**, *37*, 785−789.
(179) Becke, A. D. Density−functional thermochemistry. III. The role of exact exchange. *J. Chem. Phys.* **1993**, *98*, 5648−5652.
(180) Becke, A. D.; Johnson, E. R. A density-functional model of the dispersion interaction. *J. Chem. Phys.* **2005**, *123*, 154101.
(181) Grimme, S.; Ehrlich, S.; Goerigk, L. Effect of the damping function in dispersion corrected density functional theory. *J. Comput. Chem.* **2011**, *32*, 1456−1465.
(182) Weigend, F.; Furche, F.; Ahlrichs, R. Gaussian basis sets of quadruple zeta valence quality for atoms H-Kr. *J. Chem. Phys.* **2003**, *119*, 12753−12762.

DOI: 10.1021/acs.jctc.7b00654
J. Chem. Theory Comput. 2017, 13, 6023−6042